NREL
NATIONAL RENEWABLE ENERGY LABORATORY

Ramping Performance Analysis of the Kahuku Wind-Energy Battery Storage System

V. Gevorgian and D. Corbus

NREL is a national laboratory of the U.S. Department of Energy
Office of Energy Efficiency & Renewable Energy
Operated by the Alliance for Sustainable Energy, LLC

This report is available at no cost from the National Renewable Energy Laboratory (NREL) at www.nrel.gov/publications.

Management Report
NREL/MP-5D00-59003
November 2013

Contract No. DE-AC36-08GO28308

NREL
NATIONAL RENEWABLE ENERGY LABORATORY

Ramping Performance Analysis of the Kahuku Wind-Energy Battery Storage System

V. Gevorgian and D. Corbus

Prepared under Task No. IDHW.0370

National Renewable Energy Laboratory
15013 Denver West Parkway
Golden, CO 80401
303-275-3000 • www.nrel.gov

Management Report
NREL/MP-5D00-59003
November 2013

Contract No. DE-AC36-08GO28308

Cover Photos: (left to right) photo by Pat Corkery, NREL 16416, photo from SunEdison, NREL 17423, photo by Pat Corkery, NREL 16560, photo by Dennis Schroeder, NREL 17613, photo by Dean Armstrong, NREL 17436, photo by Pat Corkery, NREL 17721.

Printed on paper containing at least 50% wastepaper, including 10% post consumer waste.

Table of Contents

List of Figures

List of Tables

1 Introduction

High penetrations of wind power on the electric grid can introduce technical challenges because of resource variability. Such variability can have undesirable effects on the frequency, voltage, and transient stability of the grid. Energy storage devices can be an effective tool in reducing variability impacts on the grid in the form of power smoothing and ramp control. In large, interconnected power systems, the size of individual generation units is small compared to the capacity of the entire system. Therefore, a power imbalance caused by the sudden loss of a single generator is relatively small because operating reserves are shared among a large number of generators and risk to system security is minimal. The rate of change of frequency during the loss of a generator tends to be low because of high system inertia. Small, isolated island systems without interconnections are more sensitive to system disturbances because of lower inertia and higher costs of spinning reserves. The addition of a large amount of variable wind power imposes unique challenges on island power systems that large electric grids in the continental United States do not experience. The reliability of an island electric system is highly dependent on its ability to accommodate changes resulting from variability in the most economic manner while maintaining power quality and continuity of service to customers. There are several time scales of variability introduced by wind power generation that energy storage can help mitigate. With rising oil prices, stringent emission limits, continuous advances in energy storage technologies, growing technology maturity, and the development of lower-cost storage systems, energy storage is becoming an enhancing tool for the utilization of renewable energy resources in island power systems.

Integrating an energy storage system with a wind power plant can help smooth out the variable power produced from wind. Recent advances in electricity energy storage technologies provide opportunities to address wind energy variability at different time scales. The application of energy storage technology is characterized by its energy capacity (amount of energy that can be stored in the device) and power capacity (the rate at which energy can be transferred into or out of the device). The characteristics of a particular storage technology (charge/discharge rates, response times, cycle life, etc.) are also critical in determining its application range.

Several types of energy battery storage technologies have been deployed in a number of power systems throughout the world for smoothing variable power output from wind and solar power plants. Such technologies primarily include lead-acid, Li-ion, and NaS systems. In particular, several fast-response, megawatt-scale battery systems were recently deployed throughout the Hawaiian Islands to support wind and solar projects. Integrating a battery storage system with a wind power plant can help reduce power ramps of the plant output. Ramps should be limited to reduce the impact on power system reliability and allow the integration of larger amounts of variable generation with minimum high-cost ancillary service requirements from conventional generation. The size, efficiency, response time, and control strategy for an energy storage system are important parameters that contribute to a plant's ability to meet the ramp rate requirements set by the Hawaiian Electric Company (HECO). A battery system can be charged during ramp-up events and discharged during ramp-down events without wasting energy for wind curtailments (except for round-trip losses in batteries) and requiring costly reserve services by conventional generation.

2 Transmission and Distribution System in Northern Oahu

HECO operates a 138-kV transmission system in Oahu to deliver generated power to substations and distribution systems. Bulk power generated from conventional power plants is located in the Kahe and Campbell Industrial Park areas and transmitted to the East Oahu service area via two major 138-kV transmission corridors (Figure 1). The northeastern transmission corridor presently has three 138-kV transmission lines feeding power to the Koolau substation; however, only one line is in operation approaching its capacity limit [1].

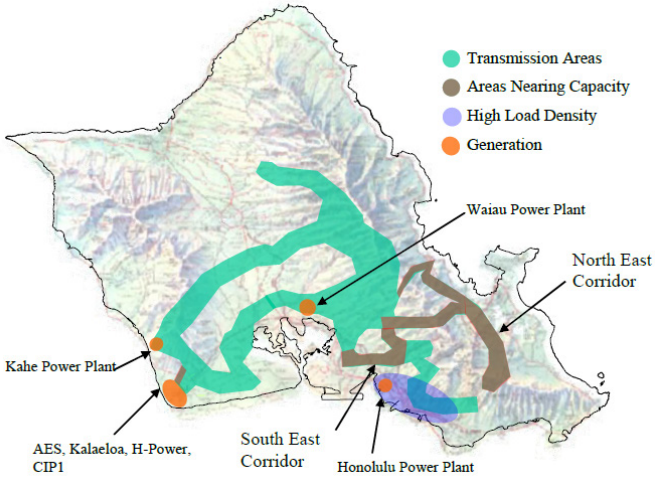

Figure 1. HECO generation and 138-kV transmission systems. ***Image from HECO***

From the transmission level, voltage is stepped down to the 46-kV sub-transmission level. The approximate locations of HECO's 46-kV sub-transmission circuits and general load areas are shown in Figure 2, in which the blue shaded areas mark 56% of HECO's total system load. The loads located in the north and northeast coastal areas are served by the 46-kV sub-transmission system, which has a much lower power flow capability than the 138-kV transmission system [1].

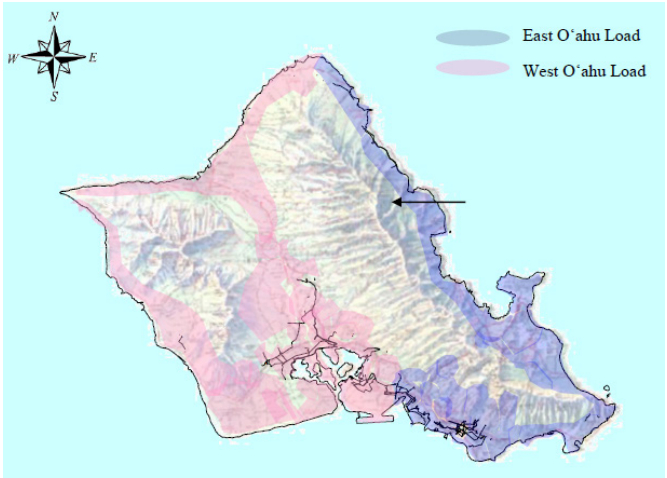

Figure 2. HECO load distribution. ***Image from HECO***

The North Shore has been identified as a location with exceptional wind resources. First Wind's Kahuku Wind Power (KWP) plant is located in the brown-shaded area shown in Figure 3. The available capacity in this area has already been filled with Kahuku and Kawailoa projects. The blue-shaded area has potential for 30 MW of wind generation capacity. The rest of the 46-kV system in the North can support only 50 MW of new generation (the areas outside of the blue- and brown-shaded areas shown in Figure 3) without transmission infrastructure upgrades [1].

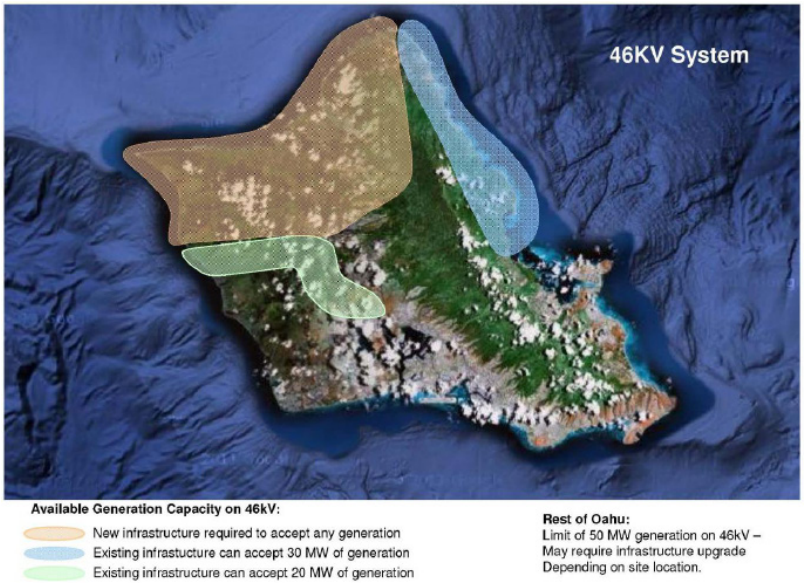

Figure 3. Available generation capacity on the 46-kV system. ***Image from HECO***

The existing 46-kV transmission infrastructure in the north is shown in Figure 4. It ties back to the 138-kV transmission system in Wahiawa. There are two 46-kV radial circuits in the area, from the Waialua substation to the Kuilima and Kahuku substations. The capacity of each of the two 46-kV circuits will be exhausted after another 20-MW wind project is added [1].

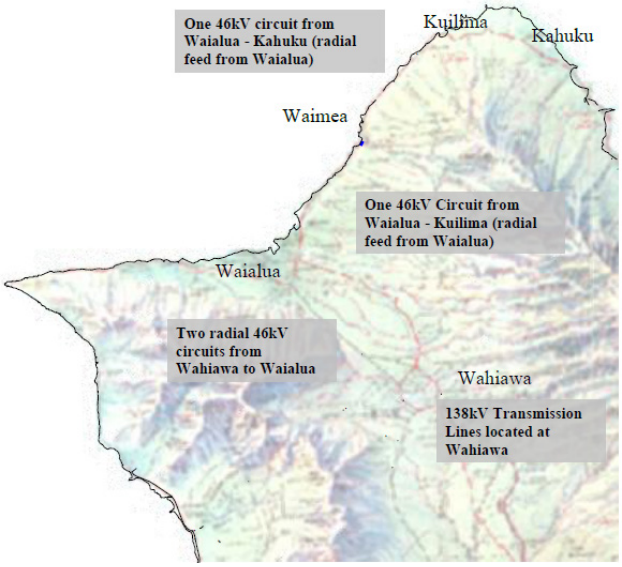

Figure 4. North Shore radial 46-kV circuits. ***Image from HECO***

3 The KWP

Located on the North Shore of Oahu (Figure 5), the KWP consists of 12 wind turbine generators rated at 2.5 MW each. The total generating capacity of the plant is 30 MW. The 2.5-MW Clipper Liberty wind turbines use variable-speed technology with full-size power conversion (known as Type 4 turbine architecture). The KWP is interconnected to the HECO 46-kV system via the Wailalua-to-Kahuku 46-kV transmission line. The two lines are in series and fed by breaker 4683 at the Wahiawa substation, and the demarcation between the two lines is at the sectionalizing breaker 4429 at the Waialua substation.

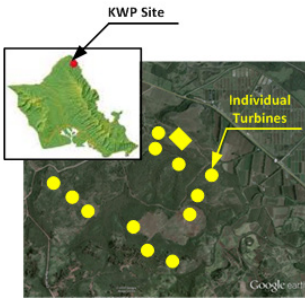

Figure 5. KWP location

HECO established requirements that wind power plant project developers must meet to qualify for interconnection. The requirements for ramp rates and potential power fluctuations as stipulated in the HECO power purchase agreement led First Wind to examine the potential for integrating an energy battery storage system into the KWP plant. In addition, the KWP site is unique in its transmission challenges, so the battery storage system helps avoid costly transmission upgrades.

The Xtreme Power energy battery storage system was selected as a suitable technology to mitigate variability of the KWP plant. It has been in service since 2011. The Kahuku site and the battery system installed inside a utility building is shown in Figure 6. The indoor area allows for another 10 MWh of storage to be installed should the wind farm be subject to future curtailment.

Figure 6. The KWP and battery storage system. *Photos from Xtreme Power*

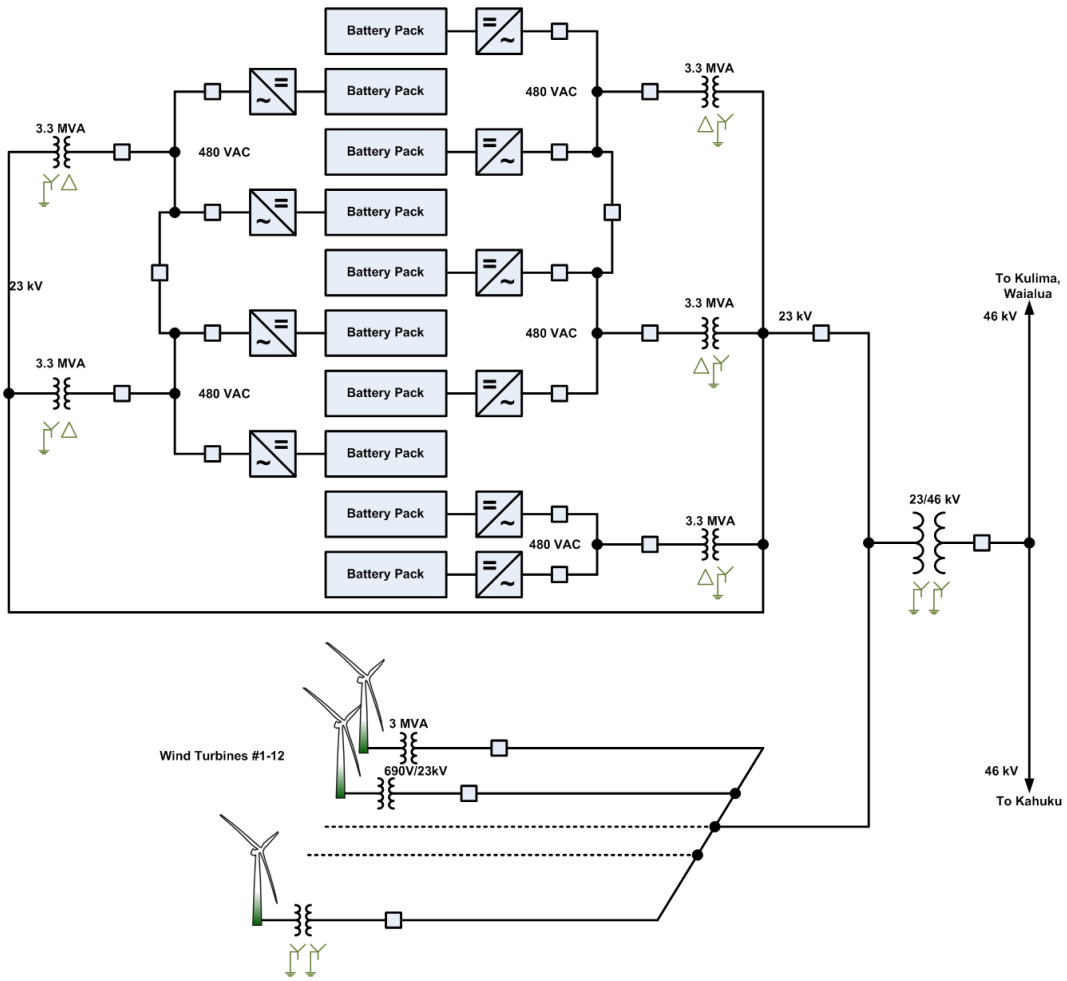

Figure 7. One-line electrical diagram of KWP

The one-line diagram of the site is shown in Figure 7. Ten 1.5-MW/1-MWh battery packs are connected to an inverter system. Pairs of inverters are connected in parallel on 480-VAC sides sharing a same 3.3-MVA transformer for stepping up the voltage to 23 kV. Twelve wind turbines are connected to the same 23-kV collector system. The whole project is interconnected with HECO's 46-kV transmission line via a single step-up transformer. The supervisory control and data acquisition (SCADA) system was set to record wind power plant and battery system active and reactive power on the 23-kV bus.

Xtreme Power's Dynamic Power Resource (DPR) is an integrated energy storage and power management system that was implemented in the KWP. DPR uses PowerCell battery technology sized to meet the interconnection requirements of the KWP plant. There are ten DPR systems with individual 480-VAC inverter/chargers capable of four-quadrant operation with simultaneous delivery or absorption of both active and reactive power. The IGBT based voltage source inverters have 1 ms subcycle response times and are capable of adjusting from a fully-rated charge to a fully-rated discharge in less than a second.

4 HECO Renewable Interconnection Requirements

HECO sets specific interconnection requirements and performance standards that projects must meet to help ensure that reliability and power quality of the Hawaiian electricity system are not compromised [1]. In particular, HECO requires limits on maximum allowed ramp rates (MW/min); defines voltage and frequency ride-through characteristics; and sets power quality, voltage regulation, and active power control requirements. HECO sets ramp rate requirements for 25-MW to 50-MW projects at 2 MW/min to 3 MW/min. The KWP power purchase agreement was negotiated in 2008 [2] and includes different upward and downward ramp interconnection requirements that vary depending on the time of the day, as shown in Figure 8.

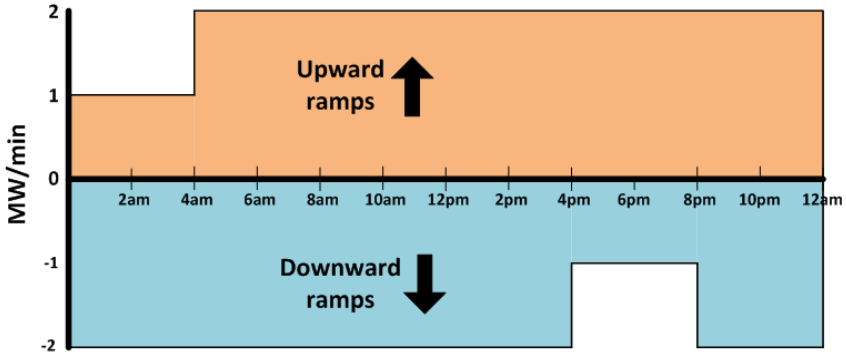

Figure 8. Ramp rate requirements for KWP

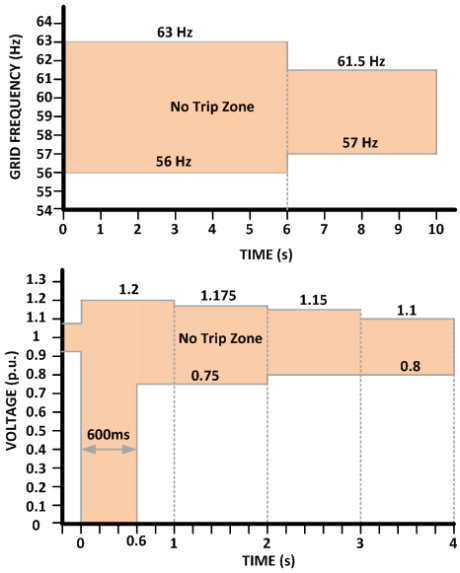

Figure 9. (Top) HECO frequency and (bottom) voltage fault ride-through requirements

HECO under-/overfrequency and voltage ride-through requirements, shown in Figure 9, define the no-trip zones during voltage and frequency disturbances. Such ride-through capabilities are important to minimize a wind power plant's impact on the transient stability of the Hawaiian power system. The individual responses of the Kahuku battery system and wind turbines to voltage and frequency excursion scenarios are shown in Table 1. The batteries are controlled to help the KWP plant meet HECO ride-through requirements under these scenarios.

Table 1. Response to Voltage and Frequency Excursions

Scenario	Battery System	Wind Power Plant
1. Overvoltage: Above 1.2 pu	Start absorbing active power to limit voltage 1.2 pu. Reduce reactive power to zero	Initiate shutdown
2. Overvoltage: 1.1–1.2 pu	No active power response. Zero reactive power output if condition persists more than 60 s	Normal shutdown if condition exists more than 5 s (ramp down at 30 MVA/12.5 s)
3. Overvoltage: 1.03–1.1 pu	No active power response. Ramp down reactive power at 1 MVAR/min	No response
4. Normal voltage bandwidth: 0.97–1.03 pu	No response	No response
5. Low voltage: 0.8–0.97 pu	No response	No response if voltage stays above 0.9 pu. Initiate normal shutdown if voltage stays below 0.9 pu for up to 3 s
6. Low voltage: 0–0.8 pu	No response until V<0.15 pu, then inject current to prop up voltage	Initiate normal shutdown if voltage stays below 0.9 pu for up to 3 s
7. Overfrequency: f>63 Hz	Zero output	Initiate normal shutdown if frequency stays above 63 Hz for more than 0.5 s
8. Normal frequency bandwidth: f = 56Hz–63Hz	No response	Initiate normal shutdown if frequency stays below 57 Hz for more than 6 s
9. Underfrequency: f<56 Hz	Zero output	Normal shutdown

Additional voltage regulation requirements under contingency scenarios were also implemented in the KWP plant control, as shown in Table 2.

Table 2. Response to System Operating Contingencies

Scenario	Battery System	Wind Power Plant
1. Wind turbine generator circuit breaker (CB) opens	Standard active power excursion control and voltage regulation	Flag low-voltage ride-through (LVRT) event, initiate LVRT shutdown
2. Battery CB opens	Zero output	Ramp down at 1 MVA/min
3. Point of interconnection circuit (POI) circuit breaker opens	Zero output	Flag LVRT event, initiate LVRT shutdown
4. Waialua Substation CB opens	Standard voltage regulation, limit voltage by absorbing power (20 MVA up to 2 s)	No response
5. Kahuku Substation CB opens	Standard voltage regulation	No response
6. Loss of communications with substations	Standard voltage regulation	No response
7. Individual wind turbine generator shutdown due to high winds	Standard voltage regulation	Go to standby state after completing shutdown
8. Multiple short-duration low-voltage events (above 0.5 pu)	Standard voltage regulation	No response

5 Methods and Formulas for Measuring Ramping Performance Metrics

HECO defines calculation methods for the following performance metrics based on measurement data obtained by the SCADA at a 2-s scan rate [2]:

- Ramp rate, *RR*
- Instantaneous power fluctuation rate, *I*
- Subminute power fluctuation rate, *A*

The ramp rate calculations are performed using the following formula:

$$RR = |MW_{i-30} - MW_i| \qquad (1)$$

Where RR is calculated for every 2-s scan and MW_{i-30} is the instantaneous MW analog value 30 scans (60 s) prior to the present scan, MW_i.

The instantaneous power fluctuation rate is calculated as

$$I = |MW_{i-1} - MW_i| \qquad (2)$$

Where I is the instantaneous power change calculated for each scan, MW_{i-1} is the instantaneous MW analog value for the previous scan, and MW_i is the instantaneous MW analog value for the present scan.

The subminute average power fluctuation rate is calculated as

$$A_1 = \frac{\sum_{k=1}^{30} |MW_{k-1} - MW_k|}{30} \qquad (3)$$

Where A_1, the subminute average power fluctuation rate, is calculated every 30 scans.

In general, a ramp event is defined as a power change event at any time interval. If the power change is positive, it is defined as a ramp-up event; it is defined as a ramp-down event if the power change is negative. The rate of power change is defined as a ramp rate calculated on a minute-to-minute basis, so the ramp rate unit is MW/min.

There are several ways in which ramp events are defined in the technical literature, as described in [4], [5], and [6]. Equation (1) above focuses on the values at the end points of each 60-s interval. Another definition is based on differences between max and min values in an interval. Ramps can also be defined as the average slope within an interval. In this analysis, all ramping and power fluctuation calculations for the KWP were done using equations (1) to (3) above.

6 Data Description

The time series data for the system was provided by Xtreme Power. The data channels recorded at the Kahuku site by First Wind SCADA system are shown in Table 3.

Table 3. Data Channels

Channel	Units	Description
Time stamp	MM/DD/YYYY hh:mm:ss	IRIG time
Active power from wind	MW	Total wind farm power
Active power to/from batteries	MW	Total AC power for all battery inverters
Total active power	MW	Total system power
RMS AC voltage – phase 1	kV	Voltage (line-to-ground) at the point of common coupling (PCC)
RMS AC voltage – phase 2	kV	Voltage (line-to-ground) at the PCC
RMS AC voltage – phase 3	kV	Voltage (line-to-ground) at the PCC
Grid frequency – phase 1	Hz	Measured from phase 1 voltage
Grid frequency – phase 2	Hz	Measured from phase 2 voltage
Grid frequency – phase 3	Hz	Measured from phase 3 voltage
Reactive power to/from wind	MVAR	Total wind farm reactive power
Reactive power to/from batteries	MVAR	Total reactive power for all inverters
Total reactive power	MVAR	Reactive power at PCC

Note: Original data units kW, volt, and kVAR were converted to MW, kV, and MVAR for convenience

Eleven-day data files were collected from November 2011, December 2011, and February 2012. Combined, the data represented 33 days of Kahuku system operation (11 consecutive days for each month). No state-of-charge (SOC) data for battery systems was provided by Xtreme Power, so all the analysis was performed without knowing the state of the batteries at any given period of time. Although both frequency and alternating current voltage were measured in each phase of the 46-kV MV line, the average three-phase voltage and frequency were calculated and used in the analysis. Figure 10 shows examples of raw data time series including the active power from the wind farm, the active AC power to/from the battery inverters, and the alternating current voltage on the 46-kV bus (line-to-ground) for each month of observation.

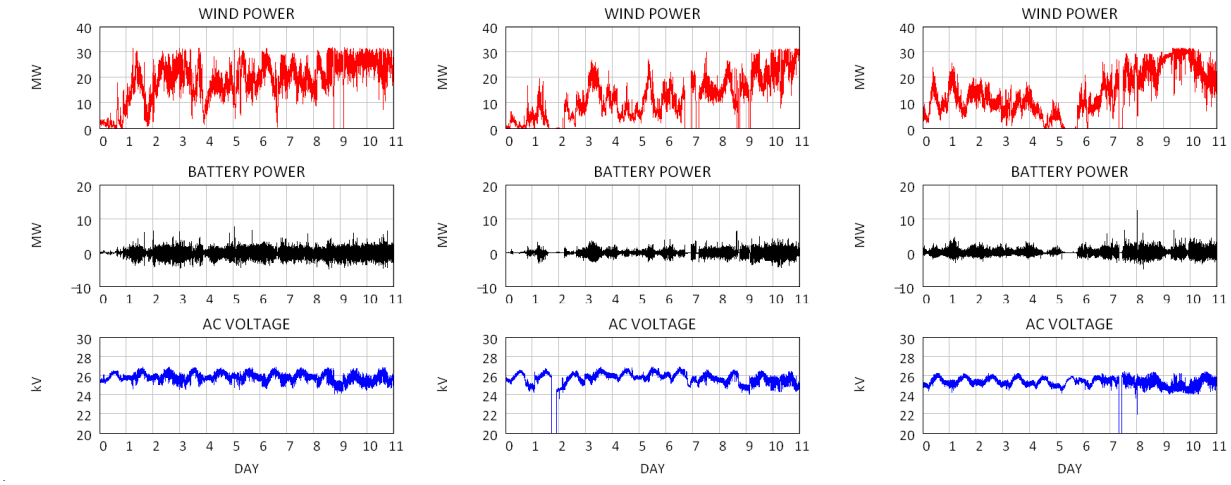

Figure 10. Examples of data for each month

The data sampling rate was expected to be at a 2-s time step. However, analysis of the time step distribution for the KWP time series showed that data time steps were not always consistently at 2 s. The frequency plot of observed time steps is shown in Figure 11, with a significant number of occurrences of time steps at different levels.

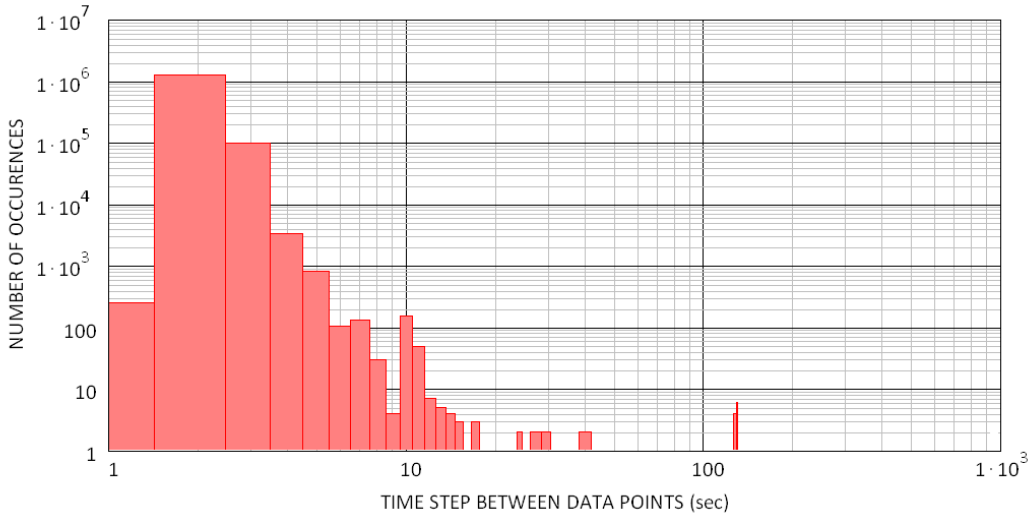

Figure 11. Distribution of data time steps

Table 4. Distribution of Time Steps

Time Step (Seconds)	Percent of Time at Level
1	0.018
2	**92.487**
3	7.151
4	0.245
5	0.06
6	0.0076
7	0.0096
8	0.0022
9	0.00029
10	0.011

As shown in Table 4 , the data sampling intervals were at 2 s during 92.5% of the observation period, and at 3 s during 7.1% of the observation period. The larger sampling intervals were observed during insignificant periods of time. The data points with only 2-s and 3-s sampling rates were filtered out and used in the analysis. The filtered data was resampled using a linear interpolation method to have a consistent 2-s sampling rate for the total observation time of approximately 790 h.

The data sets were also analyzed for grid outages during the period of observation. As shown in Table 5, there were some hours of zero voltage on the 26-kV line for Data Set #2 and Data Set #3.

Table 5. Periods of Grid Outage

Data Set	Grid Outage (h)	Grid Outage (% of time)
1 (November 2011)	0	0
2 (December 2011)	4.353	1.65
3 (February 2011)	2.61	0.988

7 Examples of 1-min Ramp Rate Limiting Performance by Xtreme Power Batteries

7.1 Ramping Performance During Normal Operation

The main purpose of the XP battery system used in the KWP project is to absorb changes in wind power plant output to limit the rate of change of power produced by the wind turbines. Such changes can be caused by the natural variability of the wind speed resource and also by contingency events in the grid, such as a sudden trip of wind turbines a result of voltage fault events or grid outages. In addition, batteries can be used to provide ramp limiting during start-ups of a wind power plant after grid outages. The XP battery system used in the KWP project was sized to meet the HECO ramp rate limits shown in Figure 8. An explanation of ramping operation of the KWP wind-energy battery storage system is illustrated in Figure 12 and Figure 13. An example 1,000-s snapshot of a 2-s active power time series was selected (Figure 12). The direction of battery active power depends on ramping behavior of the wind power plant active power output. As shown in Figure 12, batteries were being charged or discharged to limit the rate of change of wind power. In particular, batteries were charging during sustained increases in wind power (t = 100 s to 400 s) and discharging when wind power was decreasing (t = 400s to 500 s). The resulting 1-min ramp rates in Figure 13 showed a more significant reduction of the total ramps than wind-only ramps.

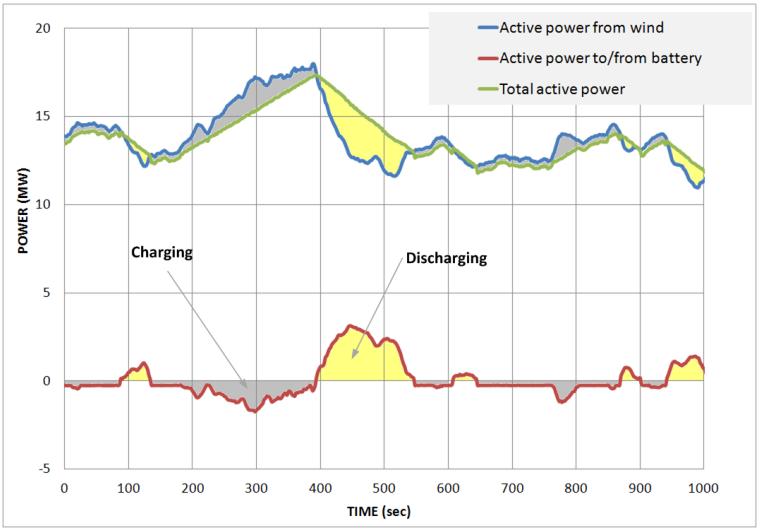

Figure 12. Snapshot of 2-s active power data

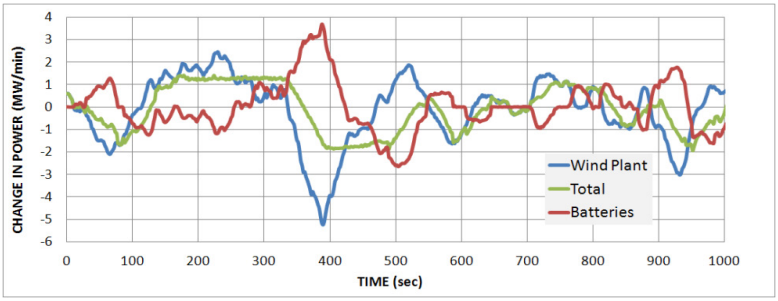

Figure 13. One-min ramping performance

7.2 Power Outage Event

Another example of a ramping event is shown in Figure 14. In this case, the whole plant was shut down because of a loss of line voltage that lasted for approximately 2.5 h. The wind power plant resumed power production shortly after grid voltage had been restored. A more-detailed view of the wind power plant start-up is shown in Figure 15. As in the previous case, the batteries began absorbing a portion of wind power plant output power to limit the total ramp rates. The resulting total ramp rates were significantly lower than the wind-only ramp rates (within ±1 MW/min), as shown in Figure 16.

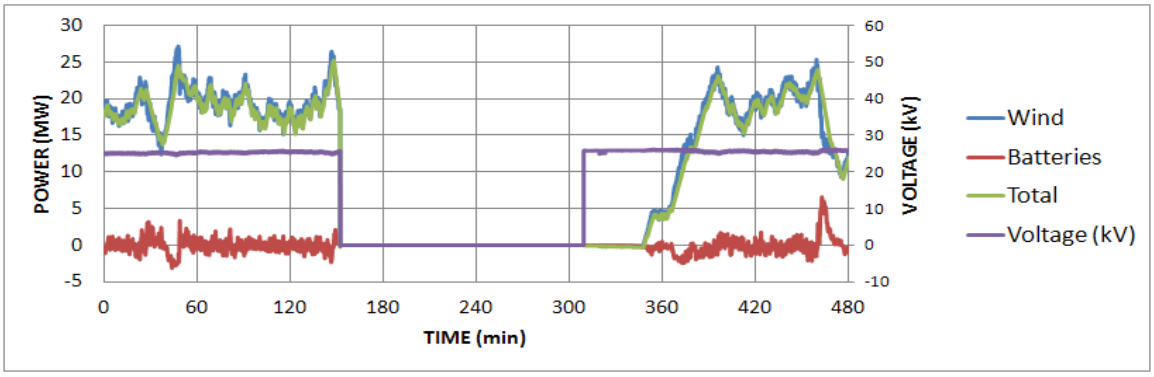

Figure 14. Example of grid power outage event

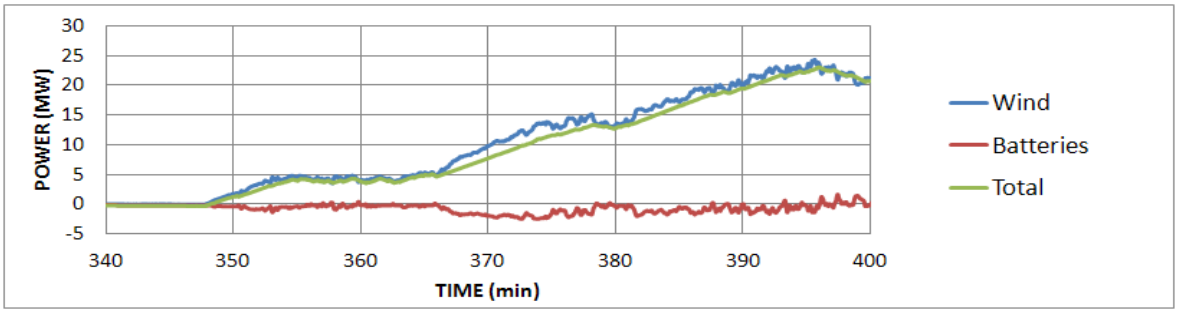

Figure 15. Plant start-up from zero power level

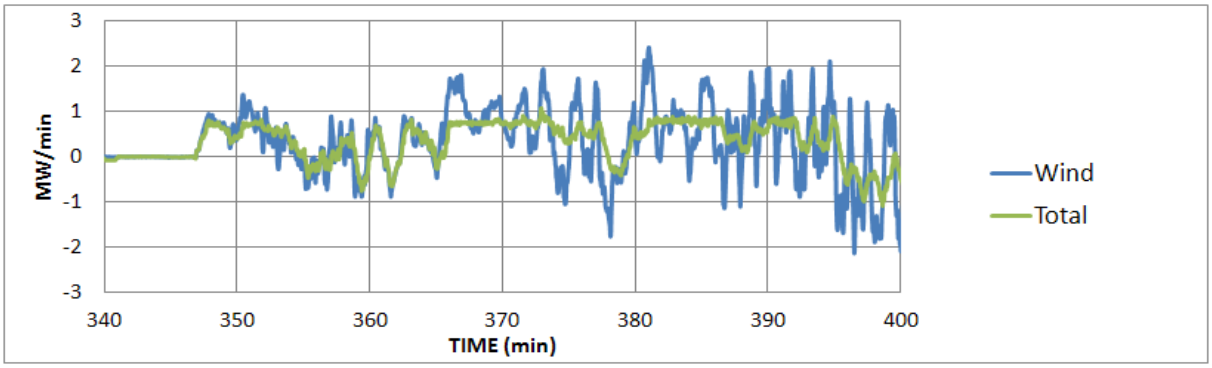

Figure 16. One-min ramp rates during the start-up

7.3 Voltage Fault Event

An interesting sequence of events demonstrating ramp limiting service by the batteries is shown in Figure 17. In this case, two consecutive, short-term, low-voltage events caused some wind turbines to trip offline. Although these low-voltage events are clearly shown in Figure 17, the real magnitude of instantaneous voltage drop is unknown because of the 2-s averaging interval.

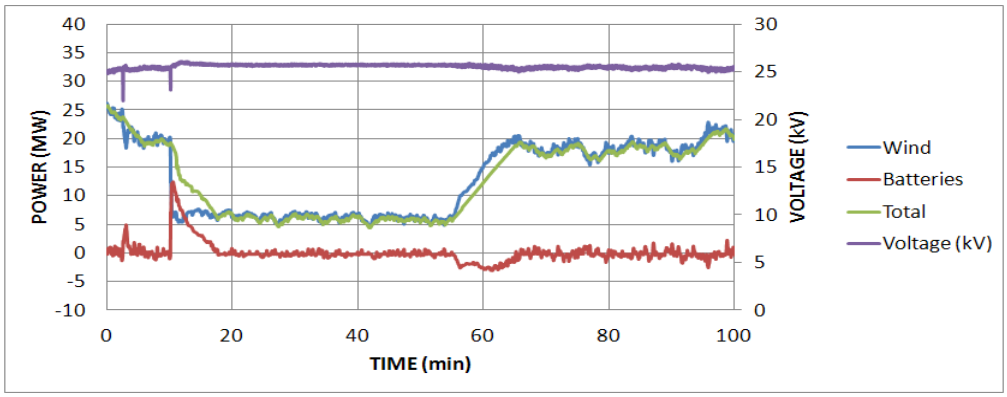

Figure 17. Loss of wind power because of grid voltage faults

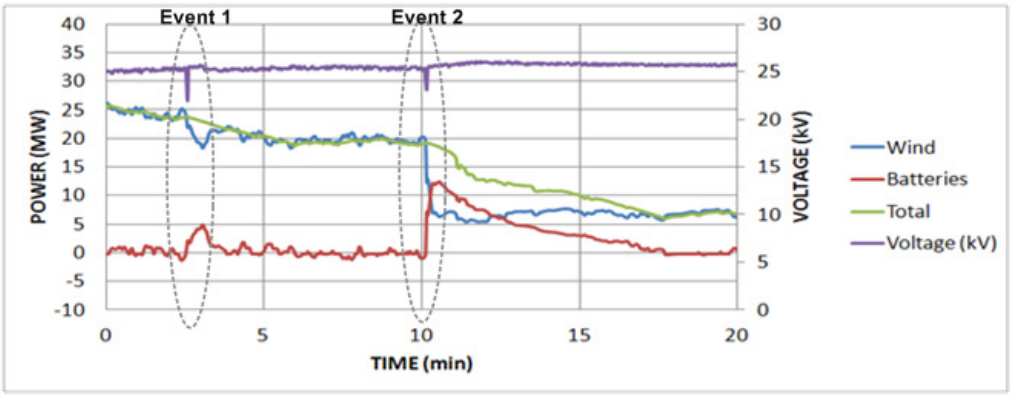

Figure 18. Detailed view of low-voltage events

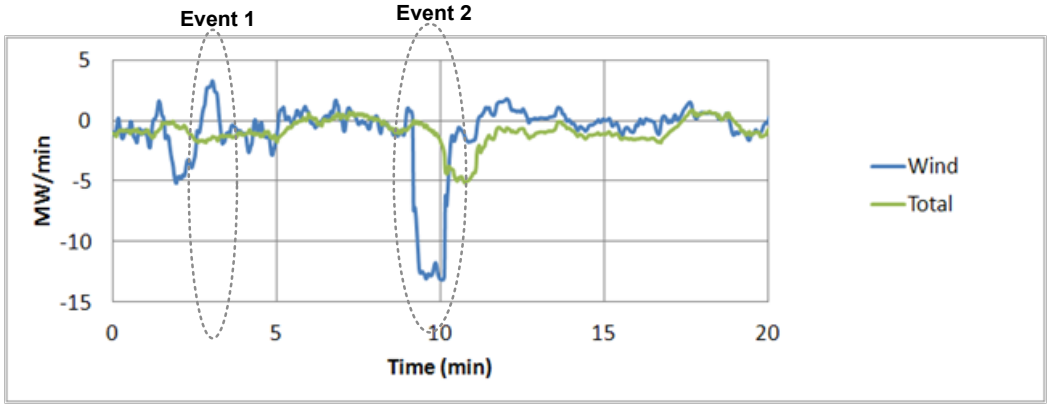

Figure 19. Resulting 1-min ramp rates

A more-detailed view of these events is shown in Figure 18. The batteries began discharging immediately after both events (Event 1 and Event 2 in Figure 18), reducing the rate of change of

total plant power. The significant reduction in the resulting ramp rates can be observed in Figure 19. In particular, in Event 2 the resulting peak ramp rate was approximately -5 MW/min; whereas it was -13 MW/min for the wind-only ramp rate. The plant returned to normal operation approximately 50 min after the event, and the batteries helped reduce the ramp-up rates, as shown in Figure 17.

7.4 Impact on Power Variability at Different Time Scales

Energy storage helps reduce variability of wind power at different time scales. To demonstrate this, we took a closer look at the negative ramping event shown in Figure 20, in which the wind power dropped from 30 MW (the rated power of the wind power plant) down to 4 MW in approximately 20 minutes. The battery control immediately responded to this event by discharging the battery to reduce the rate of change of power. Total ramping performance of the KWP plant was calculated using the three metrics expressed by equations (1), (2), and (3). The resulting 1-min ramp rates, 2-s step changes, and 1-min average step changes are shown in Figure 21, Figure 22, and Figure 23, respectively.

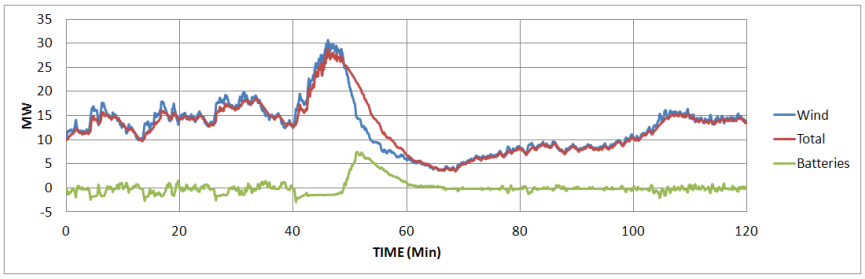

Figure 20. Negative ramp event

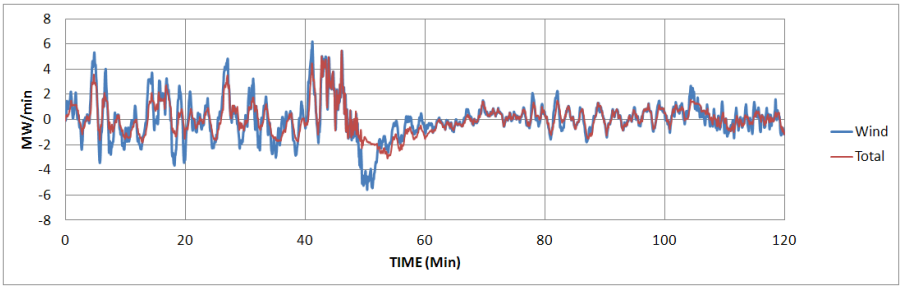

Figure 21. One-min ramp rates

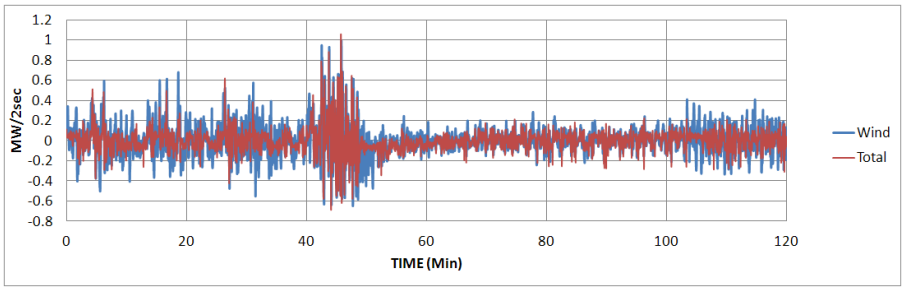

Figure 22. 2-s step changes

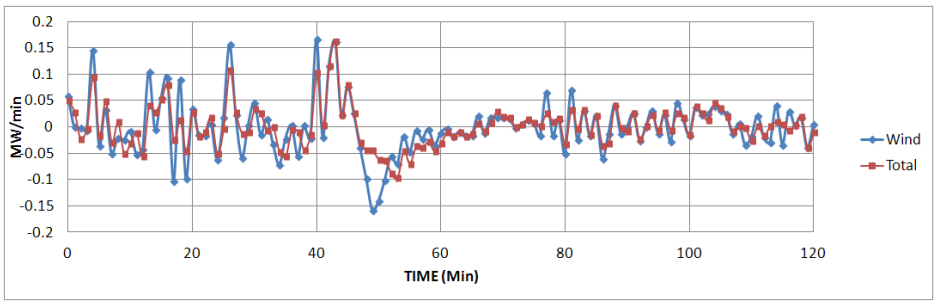

Figure 23. One-min average step changes

As shown in the figures above, the resulting rate of change of plant total output power smoother for all three cases. Although the main control objective of the battery system was to limit 1-min ramp rates, the performance improved for other metrics as well. This demonstrates the benefit of the energy storage to smooth overall variability of wind power at different time scales.

The example time series above helps demonstrate the role of XP battery storage in reducing the ramp-up and ramp-down rates of the KWP wind power plant. This achieved by increasing the charge or discharge power depending on the ramp-up or ramp-down behavior of the wind power plant. Unlike conventional generation, the batteries do not have significant ramping constraints. The limiting factors of the battery system are its power rating and energy capacity.

8 Statistical Analysis of Ramping Characteristics of the KWP Wind-Energy Battery Storage System

After the KWP data was cleaned and brought to a consistent format, we used equations (1), (2), and (3) to analyze the active power fluctuations at different time scales. Ramping events can be a significant source of uncertainty in power systems with large levels of wind power generation. Statistical analysis of historical data is important for quantifying the mitigating effects of a battery bank on both the up and down ramping of the KWP plant. Results of such analysis can be useful in developing statistical models that might offer insights into forecasting combined wind-energy battery ramps and formulating stochastic control strategies for dealing with ramping events in the HECO power system. It was not expected that the three 11-day groups of data could provide a complete picture of performance, wind resource variability, and ramping characteristics of the KWP wind-energy battery storage system. Several issues may skew the statistics, such as forced curtailments of wind power. Without wind resource data, information about individual wind turbine status, and information on battery state of charge, it is very hard to separate the events of forced curtailments from natural ramping events. Therefore, such short and limited sets of data provide only a snapshot of system operation rather than long-term statistics on combined wind-energy battery performance.

The main purpose of this analysis was to estimate the impact of batteries on a 1-min ramp rate reduction of the KWP wind power plant because strict limits on 1-min ramps were imposed by the HECO power purchase agreement. However, it was found necessary to conduct a detailed statistical analysis of 2-s power variability as well. Variability at such a fine time scale will have little impact on the operation of the HECO power system. Nevertheless, a detailed statistical evaluation of 2-s ramping performance of the wind-energy battery storage system has never been conducted in the literature and may reveal useful insights and help identify characteristics of 2-s ramp distributions. Several potential ancillary services to the HECO grid can be provided by a battery system on a second-to-second basis (such as battery system participation in primary frequency control, inertial response, and fast responsive reserves), so knowing the statistics of fast ramping behavior by the combined wind-energy battery storage subsystem can be helpful in designing optimum control algorithms for such services.

8.1 Statistical Metrics Used in the Analysis

Some statistical background that was used in the 2-s and 1-min ramp rate analysis is described in this section using [14], [15], and [16]. We used a histogram as a graphical method for displaying the shape of distribution for both power and rate of change of power data. The class intervals, or bin widths, were determined using the square-root method, which calculates the number of bins as a square root of the number of data points in the sample [13] ($N_{bins} = \sqrt{N_{data}}$). The bin widths were then calculated directly from maximum and minimum values in the data. For data sets with a large number of points, a histogram essentially resembles continuous frequency distributions because of the large number of bins.

In addition to histogram analysis, standard deviation, and mean, we applied two other statistical measures to the characterization of ramp distributions: skewness and curtosis. Skewness is a measure of symmetry (or, more precisely, the lack of symmetry) for a given data set, and is defined as

$$\gamma = \frac{\sum_{i=1}^{N}(x_i-\mu)^3}{(N-1)\sigma^3} \qquad (4)$$

Where γ is the skewness, μ is the mean, σ is the standard deviation, and $N$is the number of data points in the set. The skewness for a normal distribution is zero, and any symmetric data set should have a skewness near zero.

Kurtosis is the degree of peakedness of a distribution. It is a measure of the magnitude of the peak of the distribution, or, conversely, how fat-tailed the distribution. It is defined as

$$\kappa = \frac{\sum_{i=1}^{N}(x_i-\mu)^4}{(N-1)\sigma^4} - 3 \qquad (5)$$

In the above definition of kurtosis, data sets with a higher value of kurtosis tend to have a distinct peak near the mean and decline rather rapidly.

Correlation coefficients are used in the statistics to measure the strength of relationship between two data sets. In this analysis, we used Pearson's correlation coefficient, commonly used in linear regressions:

$$r = \frac{N(\sum xy)-\sum x \sum y}{\sqrt{(N\sum x^2-(\sum x)^2)(N\sum y^2-(\sum y)^2)}} \qquad (6)$$

Where r is the correlation coefficient and x and y are elements of data sets.

Distribution fitting is a procedure necessary for selecting a statistical distribution that best fits the wind-energy battery storage system data and allows for the development of a valid statistical model describing system operation. The best distribution that fits the data can be selected by conducting various goodness-of-fit tests. Also, histograms give an idea of the shape of distribution. However, there are additional sensitive tools for checking if the shape is close to a model. One such tool is the quantile-quantile (Q-Q) plot, by which two distributions can be graphically compared. If the samples come from the same distribution, the Q-Q plot will be linear. Later in this report, we show some distribution fitting analysis of wind battery ramping data.

It is general practice in statistical analysis of acquired time series data to remove the outliers (data points that lie an abnormal distance from other values in a sample). This is usually accomplished by removing values that are greater than a certain percentile value (for example, the 99th percentile). In this analysis, we did not perform any outlier screening in ramp rate data. The reason for this is that extreme ramp rate events that lie in the tails of observed distribution are of significant interest in the context of this work and will have an impact on power system performance.

The statistical analysis of the KWP ramping data is based on methods and assumptions that have been used in relevant technical literature [4]–[12].

8.2 Observations and Statistics on KWP 2-s Power Data Sets

This section provides a detailed statistical insight on instantaneous power fluctuation rates for the whole period of observations. We analyzed the 2-s SCADA data on active power for the wind power plant and battery system to extract information on how the battery system impacts total plant power production at this time scale. But first we present frequency distributions of 2-s power data to provide a clearer view of plant power variations during these specific periods of observation.

A frequency distribution of 2-s wind power and total plant power is shown in Figure 24 for Data Set 1 (11 consecutive days of observation in November 2011). This frequency distribution of 2-s power data was somewhat bimodal—it had two distinct peaks. The larger mode (or a major mode) was approximately 25 MW to 27 MW, and a lower mode (or a minor mode) was approximately 2 MW to 3 MW. The least frequent values between the modes happened for intermediate power levels. The frequency of the total plant power correlated well with wind power. However, the total frequency of total power production at high regions (above 27 MW) was significantly lower than for the wind power plant because the battery system was mostly absorbing power at high regions to limit ramp rates.

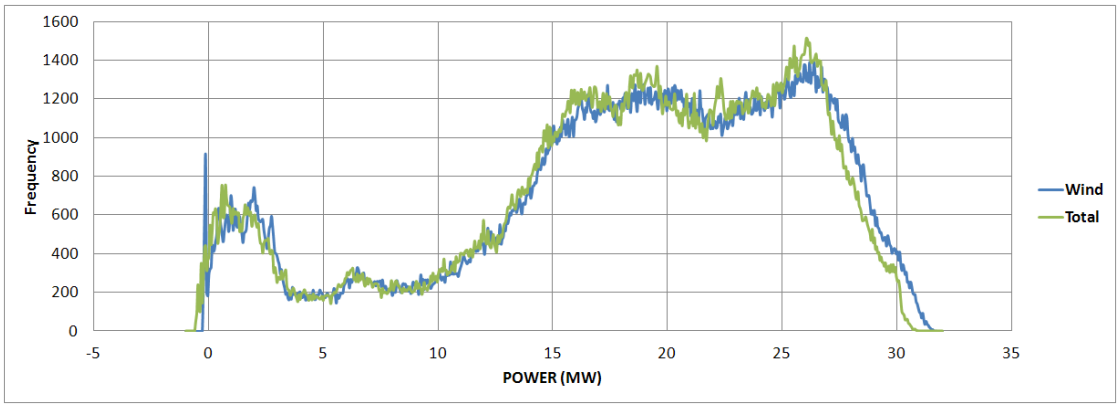

Figure 24. Frequency distribution of wind and total plant power (November 2011 data set)

In contrast to wind power, the frequency distribution of battery power was clustered around a single mode (approximately 0 MW), then extended itself with lesser frequency into tails. This is shown in Figure 25, in which the histogram for battery power was combined with wind and total power histograms. (A logarithmic scale was used on the Y-axis to reconcile the tremendous differences in the frequency of occurrences.) The distribution of the 2-s battery power was asymmetric; it had some skewness with a longer positive tail. Also, this distribution was centered on a non-zero mean. A correlation analysis between wind and battery power showed very little correlation between these two time series (Pearson's correlation coefficient = -0.129). This was an expected behavior because the control objective for the battery system was to limit the rate of change of power.

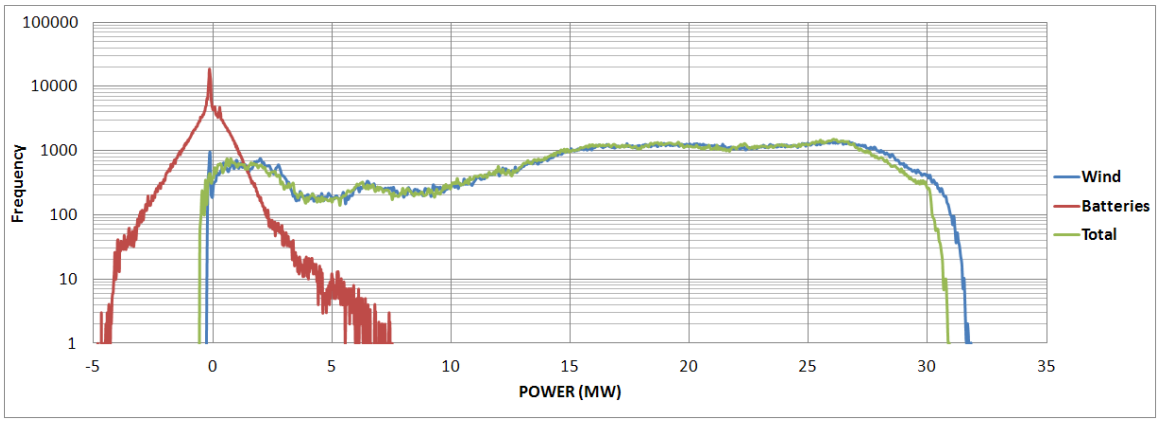

Figure 25. Combined view of frequency distributions for wind, battery, and total plant power (November 2011 data set)

A more-detailed view of the frequency distribution for battery power only is shown in Figure 26. The longer positive indicated several occurrences when the battery system was discharging at 7 MW to 7.5 MW. Conversely, the shape of the shorter negative tail indicated that the charge controller was limiting power into the batteries at approximately 4 MW to 4.5 MW. This limiting function of the controller caused the asymmetric shape in the frequency distribution for battery power. The distribution was centered around the mean value of -0.139 MW.

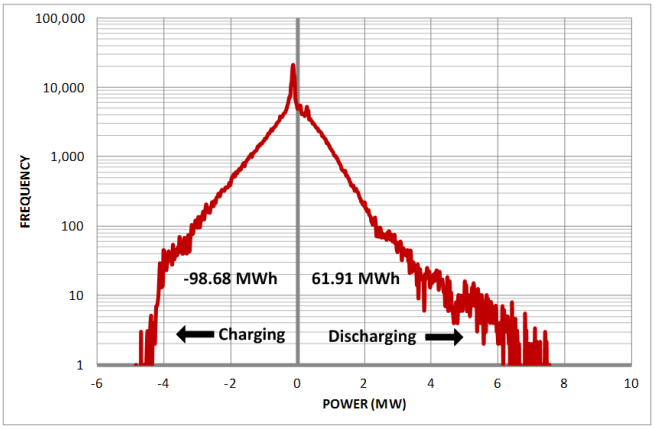

Figure 26. Detailed view of frequency distribution for battery power (November 2011 data set)

The energy to and from the battery system was calculated for the whole period of observation. For this 11-day data set, there was a total of 98.68 MWh of energy flowing into the batteries and 61.91 MWh of energy flowing out of the batteries.[1]

Table 6 lists the average, min/max, and standard deviation values of the KWP wind, battery, and total power for each of the three data sets. These results were consistent among all three data sets. The maximum recorded discharge power from the battery bank was much larger for Data Set 3; one reason is because the battery system provided a short-term surge of power during a voltage fault event (see Figure 17).

[1] It is important to note that these energy figures did not indicate and had nothing to do with MWh efficiency of the Xtreme Power battery system. They are shown here only to provide a reader with a sense of the amounts of wind energy that circulated through the battery system for this particular period of observation.

Table 6. Statistical Observations From 2-s Data Sets

MW Statistics	Data Set 1	Data Set 2	Data Set 3
Average power – wind [MW]	18.527	11.462	13.745
Average power – batteries [MW]	-0.139	-0.12	-0.127
Average power – total [MW]	18.175	11.185	13.451
Min/max power – wind [MW]	-0.263 / 31.83	-0.279 / 31.366	-0.26 / 31.62
Min/max power – batteries [MW]	-4.843 / 7.535	-4.441 / 6.337	-4.87 / 12.439
Min/max power – total [MW]	-0.556 / 30.924	-0.5 / 30.686	-1.838 / 30.675
STD – wind [MW]	7.717	8.176	8.62
STD – batteries, [MW]	0.882	0.562	0.629
STD – total [MW]	7.603	8.083	8.544
MWh to/from batteries	98.68 / 61.91	62.722 / 30.978	73.045 / 39.62

8.3 Analysis of 1-min Ramp Rates

The frequency distributions of positive and negative 1-min ramp rates (wind, batteries, and total) during an 11-day observation period in November 2011 are shown in Figure 27. These distributions were calculated for a large number of bins and are shown in logarithmic scale as a visual representation of the difference between the number of events and the large range of values. These distribution shapes were concentrated in the center, at approximately 0 MW/min, with visible tails. Table 7 lists some statistical values for the distributions shown in Figure 27. The average values for all three distributions were very close to 0. The values of standard deviation (STD) showed that 1-min total ramp rates had less variation from mean than do wind-only ramp rates. The maximum positive and negative total ramp rates were also lower than for the wind-only case.

Skewness is a measure of symmetry. The figure shows that the distributions of wind-only and total ramp rates were not exactly symmetric, with larger positive tails. In fact, the distribution for total ramp rates had a higher degree of asymmetry than did the wind-only ramps, as shown in Table 7. This is despite the fact that the distribution of battery ramp rates seemed to be far more symmetric, with a much smaller value of skewness. As shown in Figure 27, the total ramp rate distribution seemed to be symmetric for all ramp rates within a ±2-MW/min range. The asymmetrical portion of the distribution was for larger ramp rates outside of the ±2 MW/min range. This was an interesting observation, meaning that during this particular period of data collection, the combined wind-energy battery storage system produced a larger number of positive 1-min ramp rates than negative ones.

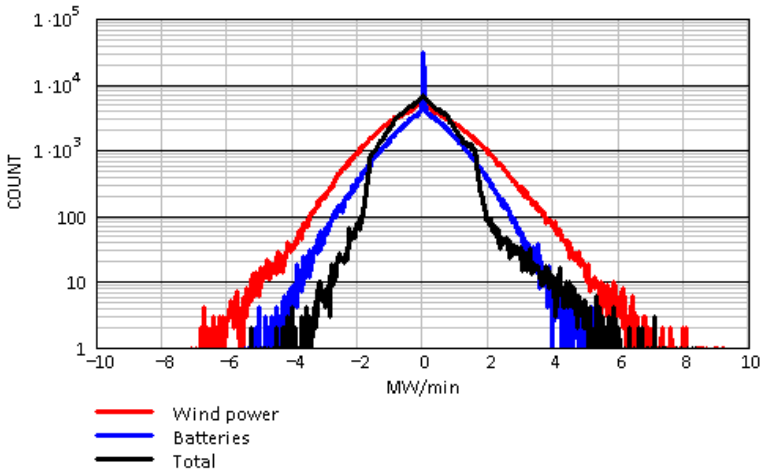

Figure 27. Distribution of 1-min ramp rates (November 2011 data set)

Table 7. One-min Ramp Rate Statistics for the November 2011 Data Set

	Wind Power	Batteries	Total
Average, MW/min	0.001	0.0011	0.001
STD, MW/min	1.258	0.024	0.781
Max positive ramp rate, MW/min	9.23 (30.7% of capacity)[1]	5.6 (37.3% of capacity)[2]	8.34 (27.8% of capacity)[1]
Max negative ramp rate, MW/min	-7.1 (23.7% of capacity)[1]	-5.47 (36.5% of capacity)[2]	-5.3 (17.7% of capacity)[1]
Skewness	0.165	-0.017	0.354
Kurtosis	1.217	1.526	1.888

1. Calculated with installed capacity of wind power plant (30 MW)
2. Calculated with installed capacity of battery system (15 MW)

Kurtosis is the measure of peakedness of distribution. Based on kurtosis values in Table 7, it appears that the distribution of total ramp rates was relatively more peaked than in the wind-only case. More-peaked distribution means higher frequency of smaller ramp rates concentrated around central axes, as shown in Figure 27.

Another observation that can be made from Figure 27 is that there was a significant reduction in the frequency of large ramping rates for total plant power (the difference between the red and black plots). More than an order of magnitude reduction in the frequency of the 1-min ramp rates was achieved for some portions of the range, and some large ramp rates were eliminated. The ratio between the frequency of wind- only and total tamp rates is shown in Figure 28 for comparison. It appeared that for a range of smaller ramp rates (±1 MW/min), there was a slight increase in the frequency of occurrences in total ramp rates compared to wind-only ones (the ratio between frequencies was less than 1). This increase was insignificant and did not impact power system operation. A small reduction in the frequency of ramp rates was observed in the range of 1 MW/min to 1.6 MW/min (both positive and negative). The frequency of larger ramp rates was reduced significantly (by a factor of 10 or higher), as shown in Figure 28, for ramp rates above ±2 MW/min.

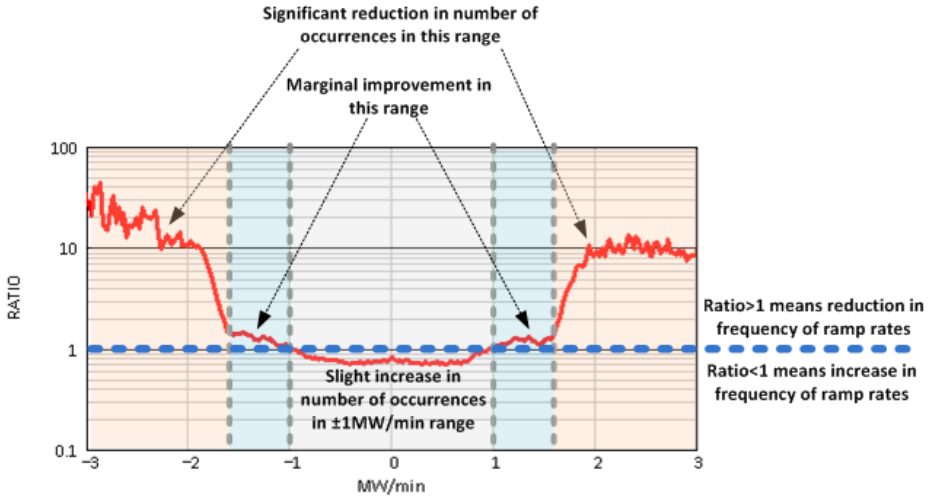

Figure 28. One-min ramp rate frequency-reduction ratio (ratio between frequencies of wind-only and total wind-energy battery 1-min ramps)

This was a significant reduction in the frequency of large positive and negative ramp rates of the 30-MW wind power plant achieved by the assistance of the 15-MW battery system. It is safe to assume that such a dramatic decrease in the number of large ramping events had a positive impact on HECO operation. In general, incremental regulation requirements by conventional generation as a result of wind power are highly correlated to the ramp rate of wind generation. Higher levels of variable wind power generation will further challenge the ramping capabilities of thermal units. The operational data from the KWP wind-energy battery storage system demonstrates that fast-response energy storage can help mitigate short-term variability and ramping of wind generation, and help wind power plants meet HECO ramping constraints.

The relative frequency of 1-min ramp rates is also shown in Figure 29, grouped in 1-MW/min bins. This representation of distribution data combined with a tabular form (Table 8) gives a better sense of the ramp rate reduction ratio for different MW/min intervals (bins). For example, approximately 35 times more reduction in the frequency of the ramp rates occurred in the bin centered at -5.5 MW/min (-5 MW/min to -6 MW/min interval). On the opposite side, there was only a factor of 4 reduction for the 5 MW/min to 6 MW/min interval because of the positive skewness in distribution. The largest reduction in positive ramp rate frequency happened in the 2-MW/min to 3-MW/min interval, as shown in Table 8.

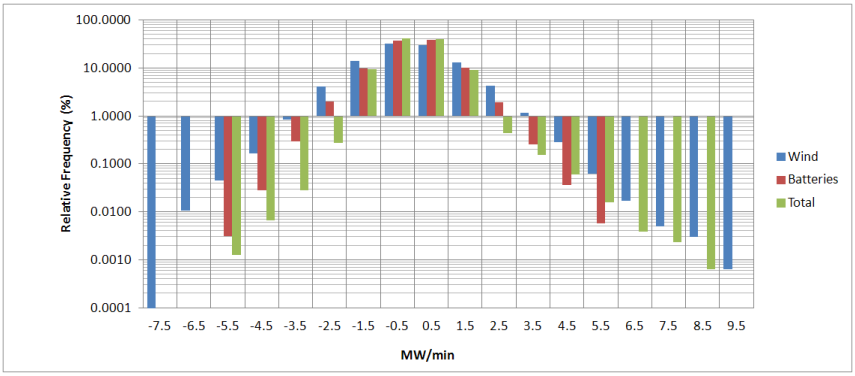

Figure 29. Relative frequency of 1-min ramp rates (November 2011 data set)

Table 8. Relative Frequency and Ramp Reduction Ratio (November 2011 data set)

	Relative Frequency of 1-min Ramp Rate Occurrences (%)			Ramp Rate Reduction Ratio
Bin (MW/min)	Wind Power[1]	Batteries	Total[3]	Ratio Between Columns 1 and 3
-7 — -8	0.0001	0.000	0.000	-
-6 — -7	0.011	0.001	0.000	-
-5 — -6	0.045	0.003	0.001	35.7
-4 — -5	0.165	0.028	0.007	24.5
-3 — -4	0.828	0.292	0.028	29.8
-2 — -3	4.133	1.971	0.273	15.1
-1 — -2	14.013	9.828	9.270	1.5
0 — -1	31.693	37.585	41.099	0.77
0 — 1	30.156	38.132	39.626	0.76
1 — 2	13.153	9.969	9.019	1.46
2 — 3	4.264	1.901	0.440	9.7
3 — 4	1.165	0.249	0.156	7.49
4 — 5	0.287	0.036	0.060	4.8
5 — 6	0.062	0.006	0.016	4
6 — 7	0.017	0.000	0.004	4.5
7 — 8	0.005	0.000	0.002	2.18
8 — 9	0.003	0.000	0.001	4.67
9 — 10	0.001	0.000	0.000	-

A similar analysis was conducted for the December 2011 and February 2012 data sets. The results and conclusion were somewhat similar to the results of the November 2011 data set analysis, and are shown in Appendix A and Appendix B, respectively.

8.4 Correlations Between Wind Energy, Battery, and Total 1-min Ramp Rates

The correlation coefficient is a measure of the strength of a linear relationship between two variables. The analysis of the linear correlation between wind-only, battery, and total ramp rates is important in trying to understand the relationship between all three and extrapolating correlations between wind power and battery operation for systems with larger capacities envisioned for the future. The scatter plot shown in Figure 30 reveals the relationship between 1-min wind-only and total ramp rates for the November 2011 data set. In this study, correlations were quantified using a simple linear correlation coefficient specified by equation (6) above. There was a moderate positive correlation (r=0.68) between wind power and total 1-min ramp rates. The decoupling effect of batteries, which were controlled to reduce the total ramp rates of the KWP plant, caused this reduced value of r. (Without batteries, $r = 1$, the ideal correlation line in Figure 30.)

A fitted linear regression identifies a positive slope in the scatter plot (slope = 0.422 with 0 intercept). The value of this slope could be used for a simplified first-order model of battery effect, and could be interpreted as a measure of wind power ramping reduction by batteries. The lower the value of the regression slope, the larger the effect of the battery system on 1-min ramp rate reduction.

The extreme outliers in Figure 30 did not have a significant impact on linear regression because they represented a small portion of total data points. More than 99% of data points fell within the shaded ±2 MW/min range,Figure 1 as shown in Figure 30. In fact, the same analysis was

performed with the outliers removed from the data (values greater than twice the 99th percentile value), with impact on the slope less than 2%.

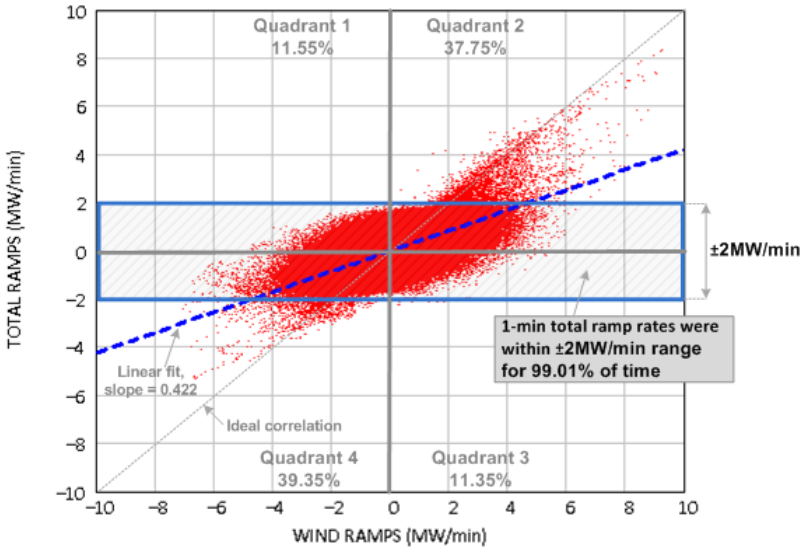

Figure 30. Scatter plot of wind-only and total 1-min ramp rates (r = 0.68)

Another interesting statistical observation from Figure 30 was achieved by analyzing the percentage of data in each quadrant of the scatter plot. The XY plain was divided into quadrants. Data points in Quadrants 2 and 4 represented total and wind-only ramp rates with the same sign (change in power in the same direction). Quadrants 1 and 3 represented data points when total and wind-only ramp rates moved in the opposite direction. There were significantly more data points in Quadrants 2 and 4 (37.75% and 39.95%, respectively) than in Quadrants 1 and 3 (11.55% and 11.35%, respectively). This means that for a significant period of time (more than 77%), the 1-min fluctuations in wind-only and total power were in the same direction. However, approximately 23% of the time, the same fluctuations were in the opposite direction.

Similar correlation analysis was conducted using the scatter plot shown in Figure 31 to understand the relationship between the 1-min ramp rates for wind-only and battery power. The data revealed stronger negative correlation between both time series (r = -0.782) than the previous case. Fitted linear regression in this case had a negative slope (-0.574). The value of this slope could also be used for a simplified first-order model of the battery effect, and could be interpreted as a measure of battery response to wind ramping. In an ideal case, the slope = -1 would provide an ideal response from the battery system. However, such response would require a larger battery and modified control strategy.

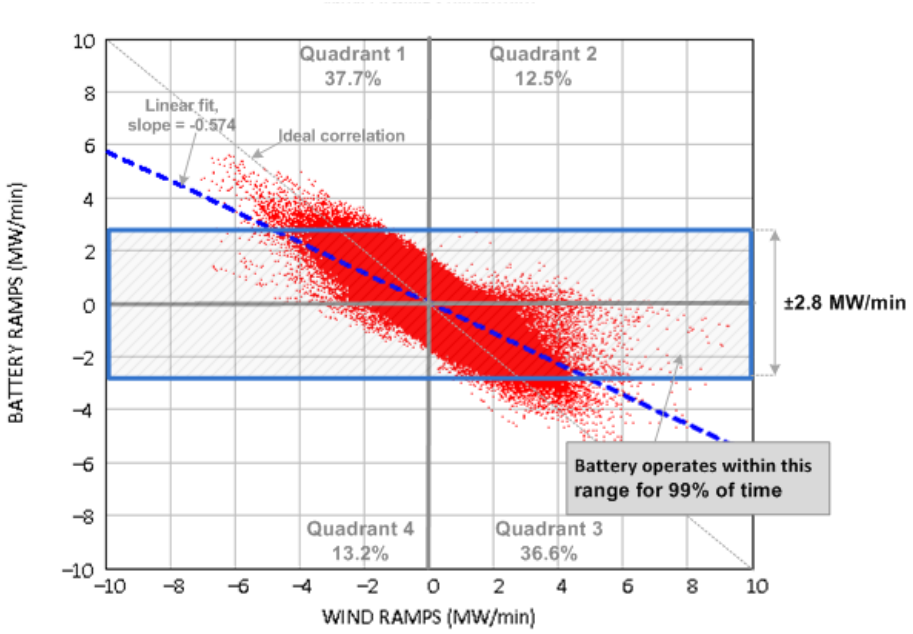

Figure 31. Scatter plot of wind-only and battery 1-min ramp rates (r = -0.782)

Analysis of the quadrant breakdown indicated that the battery system spent the most time operating in Quadrants 1 and 3 (approximately 74%), when 1-min power changes in battery output were in the opposite direction as wind power, and only 26% of the time the 1-min power changes in battery output were in the same direction as the wind power (Quadrants 2 and 4).

8.5 Segregation of 1-min Ramp Rates by Time of Day

Some periods of power system operation may be more problematic from an operational perspective because of fast changes in load. In this regard, different ramp rate limitations could be imposed on generation during certain hours of a day. HECO's 1-min ramp rate limitation schedules are as follows (and also shown in Figure 8):

- Maximum ramp rate upward of 1 MW/min during morning hours (12 a.m. to 4 a.m.)
- Minimum ramp rate downward of 1 MW/min during afternoon-evening hours (4 p.m. to 8 p.m.)
- Maximum upward and downward ramp rates of 2 MW/min for all remaining hours

In this section, we present results of ramp rate statistics segregated by hours of day, as shown above. Figure 32, Figure 33, and Figure 34 show the distribution of the 1-min ramp rates filtered for morning (12 a.m. to 4 a.m.) and evening (4 p.m. to 8 p.m.) hours for the November, December, and February data sets. These figures show the distribution of the 1-min ramp rates for wind power, battery power, and total active power of the KWP plant. In this portion of the analysis, the focus was mainly on total plant power (black histogram plots) because it determines the ability of the system to meet 1-min limitation schedules during certain hours of the day, as shown above.

Like the full data sets, for these short periods of time the average values are still close to zero. The shapes of distributions for morning and evening hours had some differences for the same

data sets, as shown in the figures below. This was most obvious in the November 2011 data set (Figure 32), in which a significant difference in the negative tails was observed between morning and evening hours. The distribution of 1-min ramp rates during morning hours was more symmetric, with similar distribution of positive and negative tails. The distribution during evening hours for the same data set had obvious nonsymmetric tails. This can be explained by the difference in the control setting of the battery system during different hours of a day. For the December and February data sets, there were no significant differences in the shapes of distributions during morning and evening hours, as shown in Figure 33 and Figure 34.

The analysis of morning and evening distributions shows that for most of the time the total 1-min ramp rates of the system were within positive and negative 1-MW/min limits, respectively. These limits were exceeded during certain percentages of the time, as indicated by the shaded areas in the black distribution plots in the figures below. The same data for each data set was consolidated in Table 9. In particular, the morning ramps exceeded the positive 1-MW/min limit during 12.9% to 19.6% of time, depending on the data set. The evening ramps exceeded the negative 1-MW/min limit during 14.4% to 25.17% of time, depending on the data set.

It is important to note that these occurrences were not interpreted as violations in this report. It is uncertain if the battery system was indeed controlled to meet the morning/evening ramp rate schedule. Thus, these were mere observations to help a reader better understand the specifics of wind-battery storage system operation.

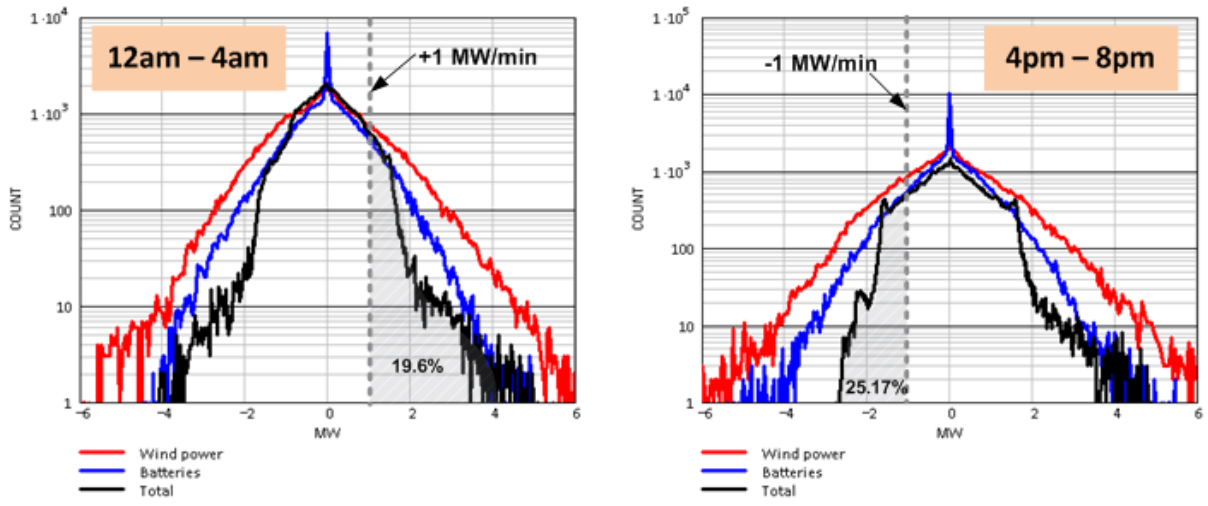

Figure 32. Morning and evening ramp rates (November 2011 data set)

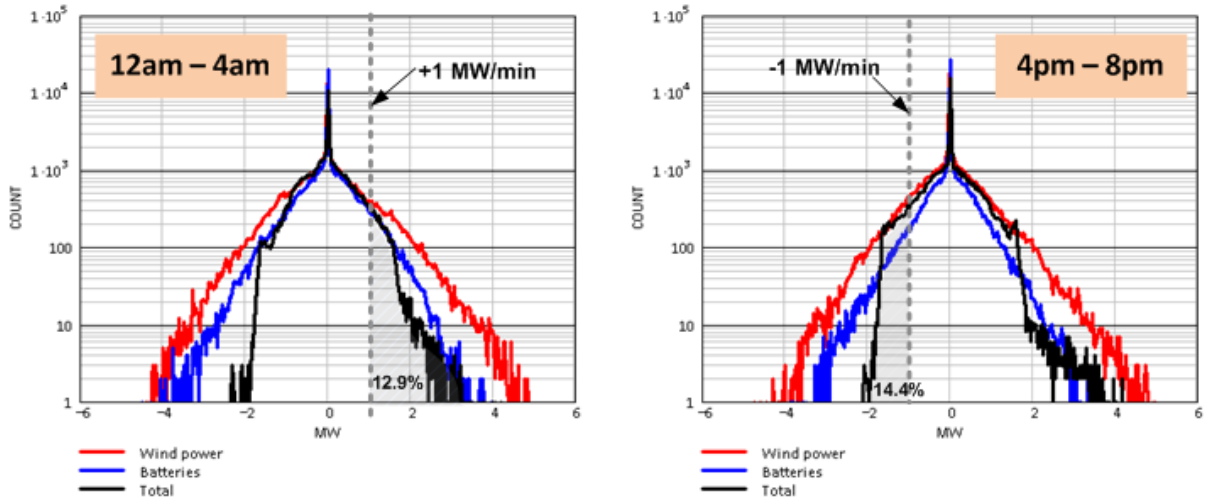

Figure 33. Morning and evening ramp rates (December 2011 data set)

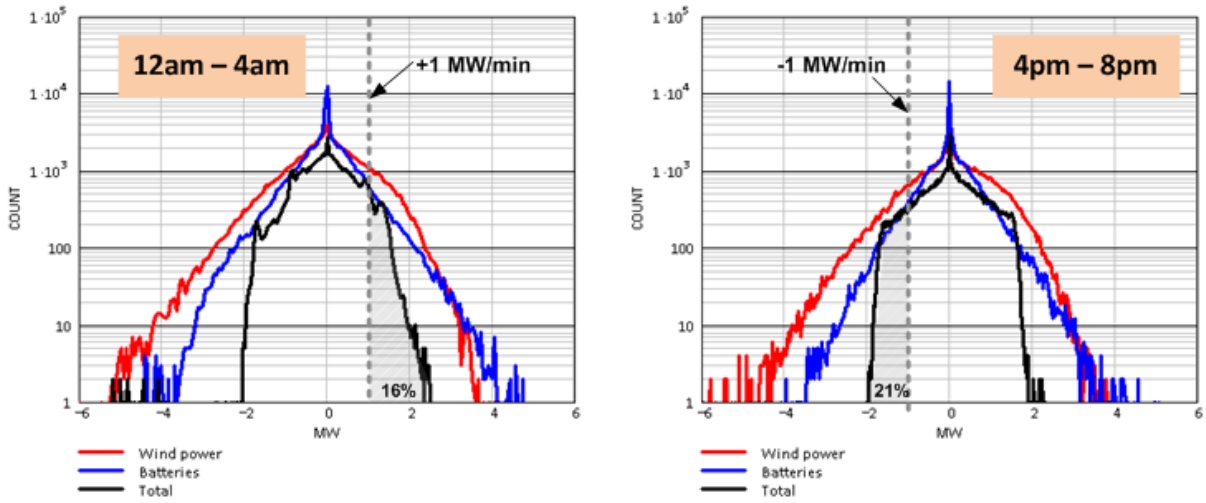

Figure 34.: Morning and evening ramp rates (February 2012 data set)

Table 9. Percentage of Morning and Evening Ramp Rates Outside of Limits

Data Set	Relative Frequency of 1-min Ramp Rates Above +1 MW/min (% of all morning Ramp Rates)	Relative Frequency of 1-min Ramp Rates Below -1 MW/min (% of All Evening Ramp Rates)
	12 a.m. – 4 a.m. +1 MW/min < Ramp Rates < +∞	4 p.m. – 8 p.m. - ∞< Ramp Rates < -1 MW/min
November 2011	19.6	25.17
December 2011	12.9	14.4
February 2012	16.01	21.03

9 Analysis of Instantaneous Power Fluctuations

Wind power can have an impact on a power system on several time scales. The variability of the KWP plant output on a second-to-second basis had a small impact on the HECO power system because such short-term changes in wind power production are small relative to the load demand and consist primarily of many uncorrelated events that change power production in different directions. The XP battery system was controlled to reduce net variability in a larger time scale (1-min ramp rates), and a reduction of second-to-second variations was not the primary control objective for the battery system. However, the battery system had an impact on the second-to-second variability of the wind power plant, even though it was not specifically controlled for this purpose during periods of normal operation. In this section, we present the analysis of 2-s power data from the KWP plant to understand the impact of the battery system on plant operations at such short time scales. Throughout the remainder of the report, we refer to fast, 2-s variability as instantaneous fluctuations, or 2-s fluctuations, to maintain consistency with HECO terms as listed in [2]. The instantaneous power fluctuations were calculated according to equation (2) above.

First, we analyzed the data to see if there was any correlation between the 1-min ramp rates and 2-s fluctuations calculated for all measured time series. The scattered plots in Figure 35 revealed weak positive correlation between the 1-min ramp rates and 2-s fluctuations for wind-only, battery, and total power, respectively. (Correlation factors are shown for each XY plot.)

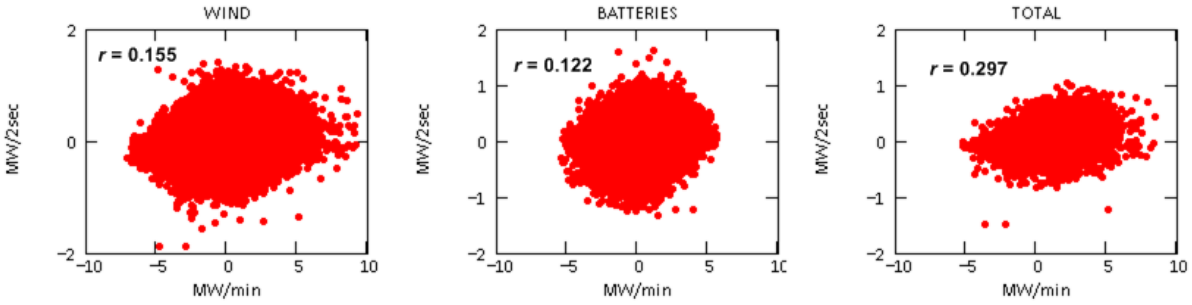

Figure 35. Scatter plots to explore the correlation between the 1-min ramp rates and 2-s fluctuations

Such weak correlations may have led to a false conclusion that the impact of batteries on 2-s fluctuations was not as strong as it was on 1-min ramp rates. However, the analysis of 2-s fluctuations in total plant power revealed a more significant reduction in frequencies than in wind-only power, as observed in Figure 36, the histogram plot of the November 2011 data set. Some statistical observations for the same 2-s fluctuations time series were consolidated and are shown in

Table 10. As in the case of 1-min ramp rates, the battery system caused an order of magnitude reduction in the 2-s fluctuations of the plant (both positive and negative), with total elimination of extreme fluctuations. The distribution of 2-s fluctuations of wind power was nearly symmetric, with little positive skewness. The distribution of 2-s fluctuations for the battery system was similar to wind, but with small negative skewnees. As shown in Figure 36, the frequency of battery power fluctuations tracked closely the frequency of wind power fluctuations for most of the range, excepting large, positive fluctuations. The distribution of 2-s fluctuations

in total plant power was symmetric for most of the range, with large, positive skewness in the tails area, and was much narrower, with a higher degree of peakedness (larger kurtosis) than the wind-only and battery distributions. As shown in Figure 36, the operation of the battery system caused some increase in frequency of small 2-s fluctuations in total plant power (within ±0.1-MW/2-s range). However, there was a dramatic reduction in the frequency of the 2-s fluctuations for the rest of the range. The majority of extreme 2-s fluctuations in total power were within ±0.5-MW/2-s range (with few outliers outside of this range).

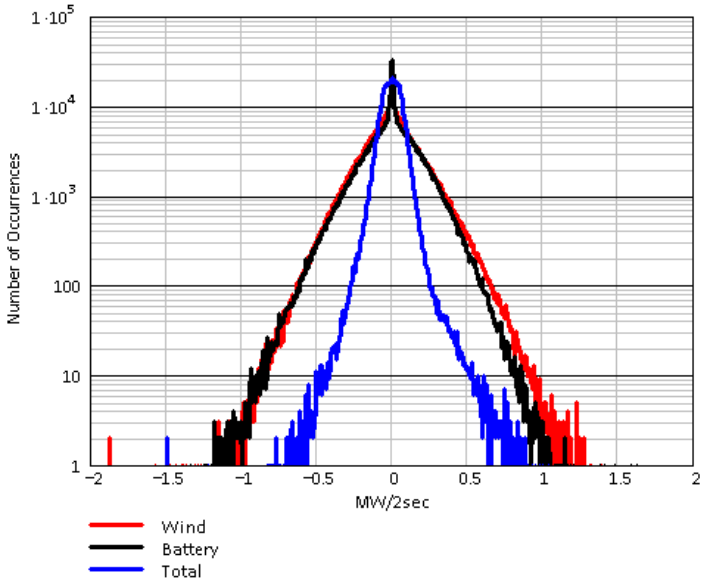

Figure 36. Distribution of instantaneous power fluctuations (November 2011 data set)

Table 10. Statistical Observations for 2-S Power Fluctuations

	Wind Power	Batteries	Total
Average, MW/2 s	0	0.	0
STD, MW/2 s	0.197	0.181	0.071
Max positive ramp rate, MW/2 s	1.41 (4.7% of capacity)[1]	1.63 (10.8% of capacity)[2]	1.04 (3.47% of capacity)[1]
Max negative ramp rate, MW/2 s	-1.87 (6.2% of capacity)[1]	-1.33 (8.8% of capacity)[2]	-1.49 (4.9% of capacity)[1]
Skewness	0.134	-0.104	0.251
Kurtosis	1.837	2.279	8.782

1. Calculated with installed capacity of wind power plant (30 MW)
2. Calculated with installed capacity of battery system (15 MW)

The scatter plot in Figure 37 shows strong negative correlation between the 2-s fluctuations in wind and battery power (correlation coefficient r = -0.945). The slope of linear fit is equal to -0.873, which can be used as a simple regression model for evaluating fast changes in battery power in response to fast wind power variability. The histogram in Figure 38 shows the distribution of frequencies in the differences between the 2-s fluctuations in battery and wind power. These differences could be interpreted as a statistical measure of how close the battery system is tracking the 2-s fluctuations in wind power. For example, if the difference were equal or close to zero, then for each MW/2 s in wind power, there would be a same change in battery power, but in the opposite direction.

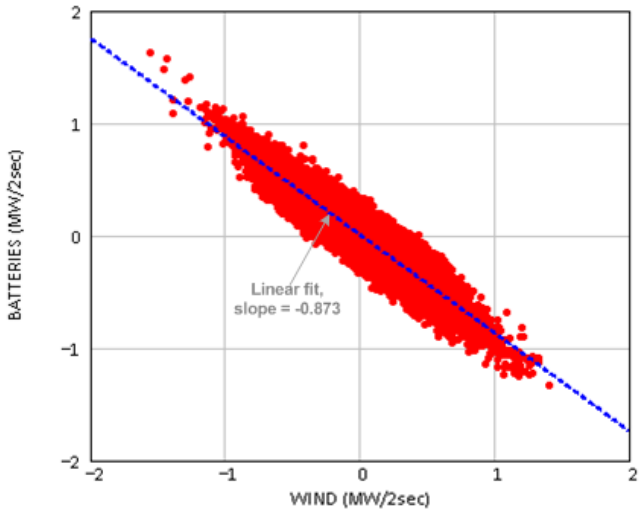

Figure 37. Correlation between 2-s fluctuations in wind and battery power (r = -0.945)

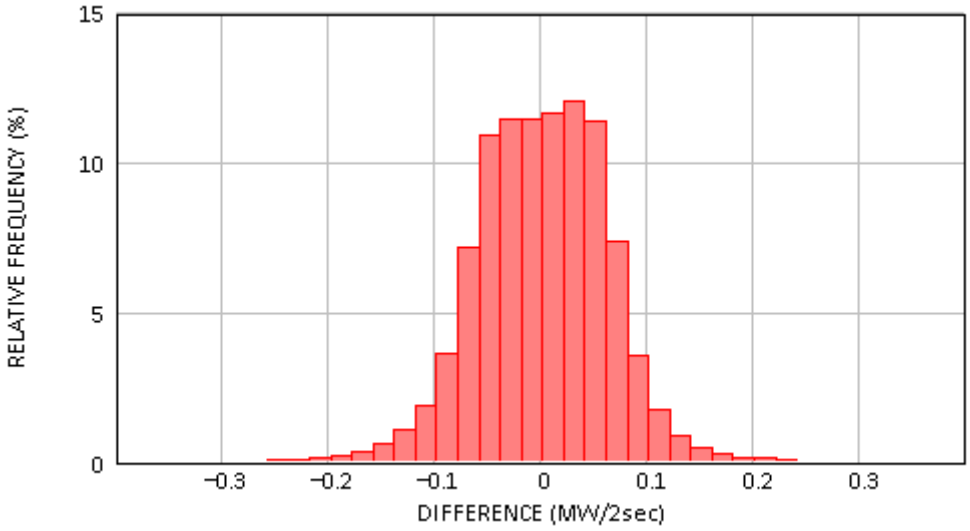

Figure 38. Distribution of differences (shows how well the battery tracks 2-s fluctuations in wind power)

10 Characterization of Ramp Rate Distributions

In this section, we analyzed the character of distributions of the 1-min ramp rate data from the KWP wind-battery system. The goal of the analysis was to examine the ramp rate data to understand which statistical distribution best fits the measured data sets and could be used to describe it. In previous chapters, we discussed shapes and other characteristics of ramp rate distributions for wind, battery, and total power of the plant. These distributions were presented in logarithmic scales for better visualization of tail events. Figure 39 shows the same distributions in normalized scale (red plots) compared to three different continuous probability distribution functions (Laplace, hyperbolic, and normal). A closer look at the distribution of measured ramp rates (red plots in Figure 39) revealed sharp symmetric peaks that were typical to the Laplace distribution.

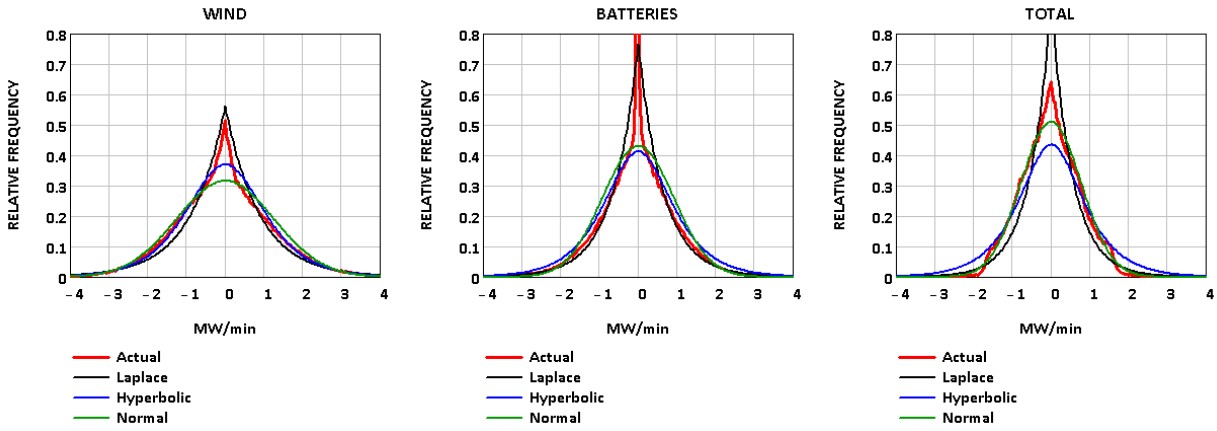

Figure 39. Comparison of measured and empirical distributions

The probability density function (PDF) of the Laplace distribution is as follows

$$f_L(x) = \frac{1}{\sqrt{2}\sigma} e^{-\frac{\sqrt{2}|x-\mu|}{\sigma}} \qquad (7)$$

Where μ and $\sigma$are the mean and standard deviation, respectively.

After preliminary analysis of several other continuous PDFs, we included two other functions in the analysis that best described the measured data for a comparison. The functions we used are the PDFs for hyperbolic and normal distributions. The PDF for hyperbolic distribution can be written as

$$f_h(\mu, \alpha, \beta, \delta, x) = \frac{\sqrt{\alpha^2-\beta^2}}{2\alpha\delta K_1(\delta\sqrt{\alpha^2-\beta^2})} e^{-\alpha\sqrt{\delta^2+(x-\mu)^2}+\beta(x-\mu)} \qquad (8)$$

Where $K_1(\delta\sqrt{\alpha^2-\beta^2})$ is modified Bessel function of the third kind with index 1, α and β are two parameters that determine the shape (steepness and skewness, respectively), μ is the mean, and δ is the scale parameter ($\delta = \sigma$).

The normal continuous PDF is defined by the formula

$$f_n(x) = \frac{1}{\sqrt{2\pi}\sigma} e^{-\frac{(x-\mu)^2}{\sigma^2}} \qquad (9)$$

The frequency distribution of actual measured ramp rates was compared to three continuous PDFs, as shown in Figure 39. The depicted hyperbolic distribution plots used the following set of shape parameters ($\alpha = 1.5$ and $\beta = 0$).

A single "candidate" distribution that best matched the data was selected for each 1-min ramp rate data. In particular, we selected the hyperbolic distribution for wind-only, Laplace distribution for battery, and normal distribution for total ramp rates. The comparison of actual and empirical cumulative distribution functions (CDF) is shown in Figure 40.

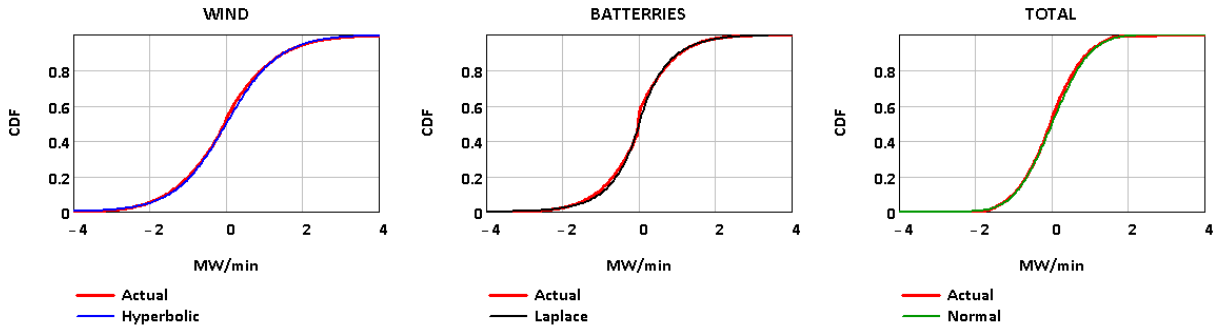

Figure 40. Comparison of measured and candidate CDFs

Such representation provided a general understanding of shape comparisons but carried very little information on how well the candidate distribution fit the measured data. In further analysis, we used other graphical means to compare two distributions. In particular, a P-P (probability-to-probability) plot can be useful tool for assessing how closely two data sets agree by plotting two cumulative distribution functions against each other (Figure 41).

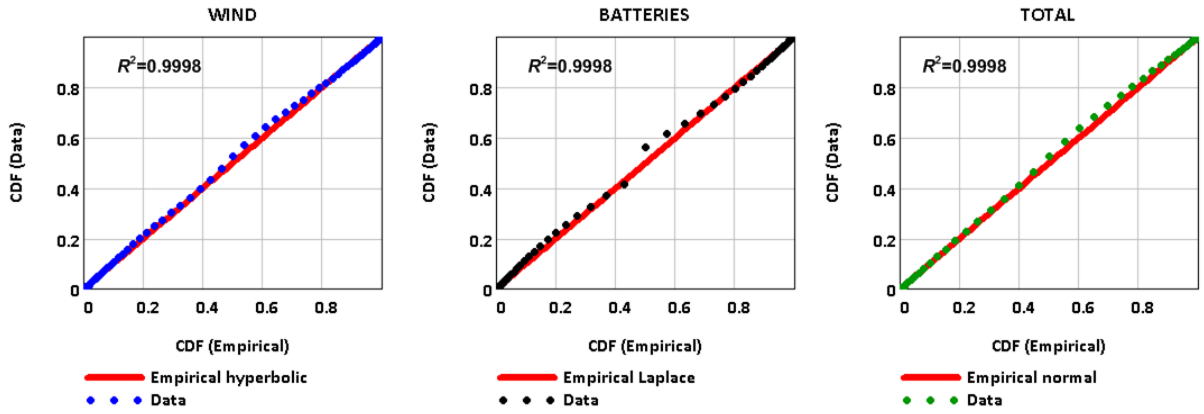

Figure 41. P-P plots

The P-P plots were expected to be approximately linear if the specified theoretical distribution was the correct model. The regression analysis (R^2 value) showed very strong linear fit between empirical and actual CDFs. As observed in Figure 41, the P-P plots were more sensitive to

discrepancies in the middle part of the distribution. These discrepancies were more obvious for battery CDFs because of the highly peaked shape of battery PDF as shown in Figure 40. The R^2 value of the P-P plots was a useful parameter for evaluating goodness to fit, but not definitive. It gave an idea of how well the data fit the model, but did not give any information on whether the model was correct.

Another graphical technique for determining if two data sets have a common distribution is based on using the Q-Q (quantile-quantile) plots. A Q-Q plot is a graph of the quantiles of the observed data plotted against the quantiles of the empirical distribution. Two distributions are similar if the Q-Q plot follows a linear pattern of a 45-degree reference line. Many distribution characteristics can be tested with Q-Q plots, particularly the presence of outliers in the sampled data.

Figure 42 shows Q-Q plots comparing the quantiles of measured 1-min ramp rates with theoretical quantiles. The plotted points were close to linear, with some outliers at the ends of the ranges. Otherwise, the data fit the selected candidate models well.

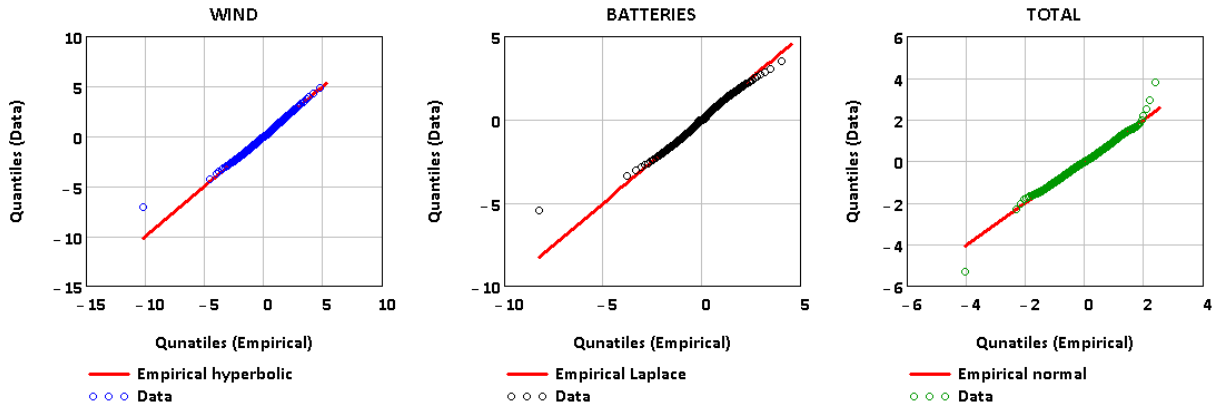

Figure 42. Q-Q plots

There are other goodness-of-fit tests that reveal information if a given distribution is not significantly different from the hypothesis (for example, Kolmogorov-Smirnov and Chi-square tests). It was not a purpose of this work to perform a complete set of stringent statistical analysis for distribution fitting. In particular, special efforts are need to devise methods for fitting the empirical distribution shapes in the tails of measured ramp rate distributions. Longer observation periods and more information about battery control set points are needed to understand and characterize the nature of outliers, which is subject of future work. The simple analysis of distribution fitting above helped identify and characterize the types of empirical distributions that best represented the operation of the KWP wind-battery system.

11 Conclusions

In this study, we provided a detailed analysis of the ramping performance of the Kahuku wind-battery system. The KWP plant is one of the largest wind battery system that has been deployed in the United States to date. The presented analysis is the first detailed insight into minute-by-minute ramping performance of a utility-scale battery system coupled with a multi-MW wind power plant based on actual field data. The results of this study can be used by HECO and other island utilities in their future wind power expansion plans, and also by large mainland utilites that plan on using similar battery systems.

The primary purpose of the Kahuku storage system is to limit ramp rates of the net production of the plant. We have examined ramping performance of the KWP plant in 1-min time scales and identified more-significant reduction in 1-min ramp rates in net plant power than wind-only power. The most obvious benefits of the battery system are a significant reduction in frequency of large positive and negative ramp rates of the 30-MW wind power plant achieved by the assistance of a 15-MW battery system. It is safe to assume that such a dramatic decrease in the number of large ramping events has a positive impact on HECO operation. In general, the incremental regulation requirements by conventional generation caused by wind power are highly correlated to the ramp rate of wind generation. Higher levels of variable wind power generation will further challenge the ramping capabilities of the thermal units. The operational data from the KWP wind-battery system demonstrates that fast-response energy storage can help mitigate short-term variability and ramping of wind generation, and help wind power plants meet HECO ramping constraints. The analysis demonstrated significant reduction in 2-s power fluctuations as well.

The analysis examined the ramp rate data to understand which statistical distribution best fits the measured data sets and can be used to describe it. It was demonstrated that the Laplace distribution best describes the 1-min ramping performance of the battery system, whereas the normal distribution best fits the 1-min ramping characteristics of net plant power.

The current work suggests a number of directions for further examination. The analysis can be expanded to include data on battery system SOC to better understand impacts of such operation on battery life and performance, capability of battery controls to manage its target SOCstate of charge, and related efforts. Also, access to control parameters of the battery system will improve interpretation of the performance of the system in different regions of operation (extreme events in particular). The authors gratefully acknowledege the contributions of Xtreme Power and First Wind for supplying the data used in the study.

12 Acknowldegments

We would like to acknowledge Bill Parks of the U.S. Department of Energy (DOE), who provided leadership for our efforts in Hawaii. We would also like to thank Dr. Imre Gyuk for his continuous leadership of the U.S. DOE storage research program. Last, but not least, we would like to thank Jennifer DeCesaro of the U.S. DOE Office of Energy Efficiency and Renewable Energy Integrated Deployment Program for supporting our work.

The authors also wish to express thanks to Marc Matsuura of HECO, Thomas Siegel of First Wind, and Alex Scorcz of Xtreme Power for data and other valuable input to this work.

13 Appendix A: Analysis of December 2011 Data Set

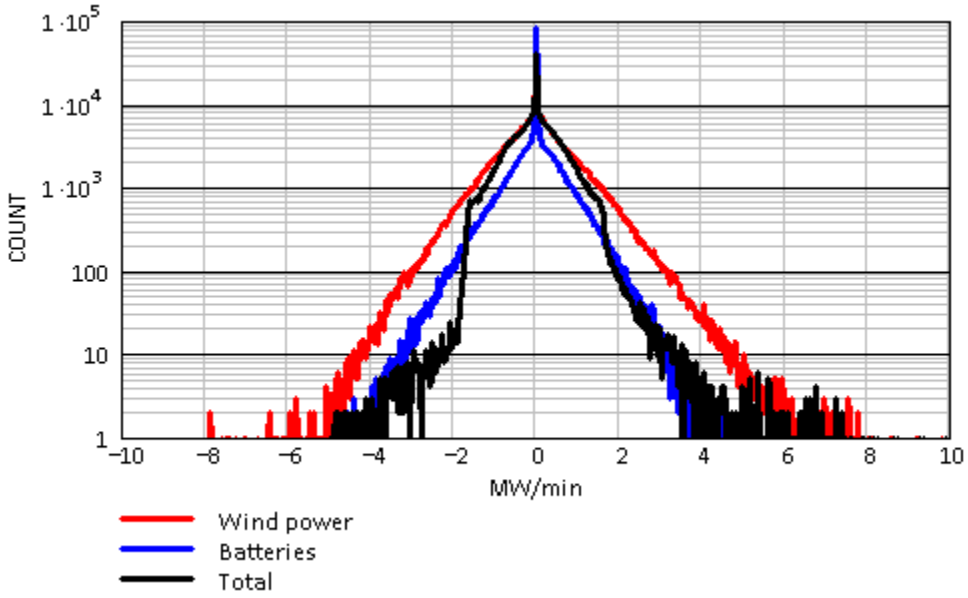

	Wind Power	Batteries	Total
Average, MW/min	0.002	0	0.002
STD, MW/min	0.942	0.626	0.652
Max positive ramp rate, MW/min	10.01 (33.3% of capacity)[1]	5.17 (34.5% of capacity)[2]	10.01 (33.4% of capacity)[1]
Max negative ramp rate, MW/min	-7.9 (26.3% of capacity)[1]	-4.87 (32.4% of capacity)[2]	-4.95 (16.5% of capacity)[1]
Skewness	0.24	-0.071	0.448
Kurtosis	3.335	4.61	4.624

1. Calculated with installed capacity of wind power plant (30 MW)
2. Calculated with installed capacity of battery system (15 MW)

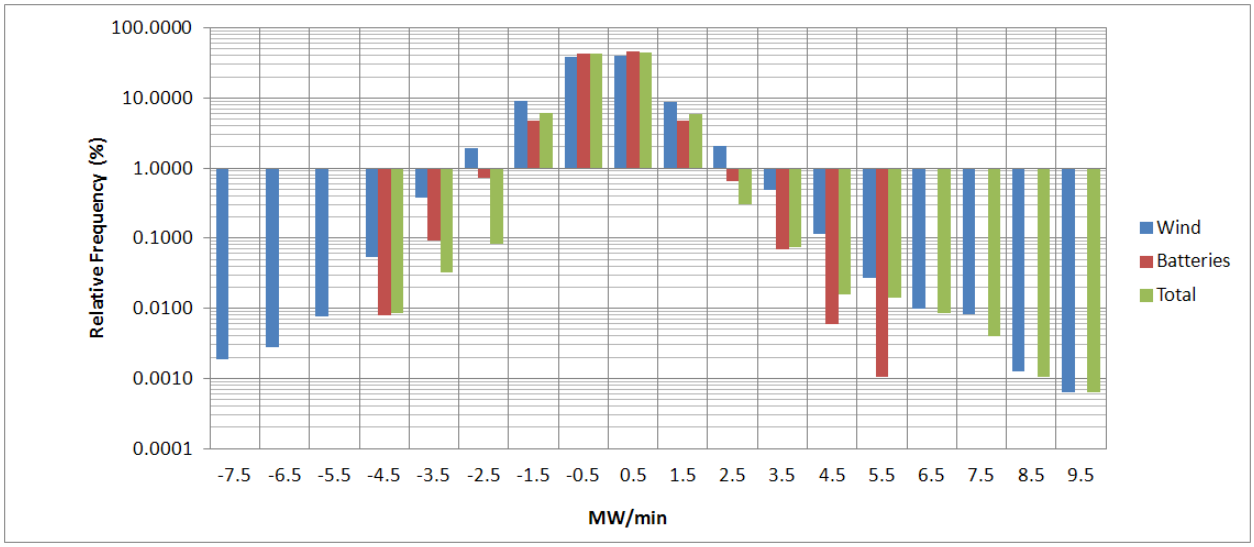

	Relative Frequency of 1-min Ramp Rate Occurrences (%)			Ramp Rate Reduction
Bin (MW/min)	Wind Power[1]	Batteries	Total[3]	Ratio Between Columns 1 and 3
-7 — -8	0.002	0.000	0.000	-
-6 — -7	0.003	0.000	0.000	-
-5 — -6	0.008	0.000	0.000	-
-4 — -5	0.055	0.008	0.009	6.34
-3 — -4	0.380	0.093	0.033	11.64
-2 — -3	1.906	0.721	0.081	23.40
-1 — -2	9.015	4.713	5.985	1.51
0 — -1	37.962	42.630	43.182	0.88
0 — 1	39.225	46.354	44.403	0.88
1 — 2	8.746	4.753	5.882	1.49
2 — 3	2.061	0.653	0.307	6.71
3 — 4	0.478	0.068	0.074	6.42
4 — 5	0.115	0.006	0.016	7.39
5 — 6	0.027	0.001	0.014	1.92
6 — 7	0.010	0.000	0.008	1.15
7 — 8	0.008	0.000	0.004	2.05
8 — 9	0.001	0.000	0.001	1.20
9 — 10	0.001	0.000	0.001	1.00

14 Appendix B: Analysis of February 2012 Data Set

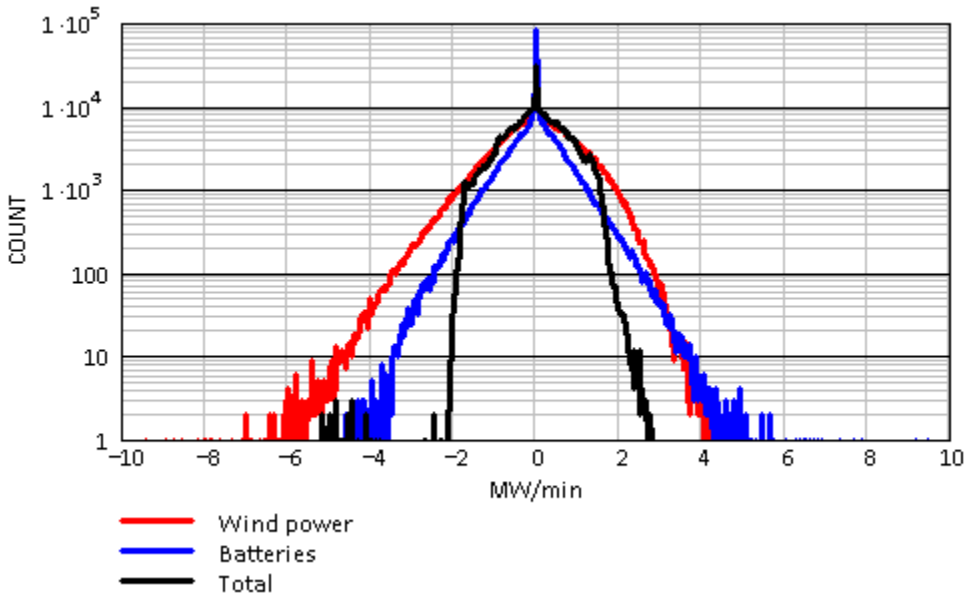

	Wind Power	Batteries	Total
Average, MW/min	0	0	0
STD, MW/min	1.01	0.713	0.717
Max positive ramp rate, MW/min	4.77 (15.9% of capacity)[1]	12.67 (84.5% of capacity)[2]	2.8 (9.33% of capacity)[1]
Max negative ramp rate, MW/min	-19.03 (63.4% of capacity)[1]	-4.83 (32.2% of capacity)[2]	-19.86 (66.2% of capacity)[1]
Skewness	-0.866	0.374	-1.255
Kurtosis	9.99	7.28	30.564

1. Calculated with installed capacity of wind power plant (30 MW)
2. Calculated with installed capacity of battery system (15 MW)

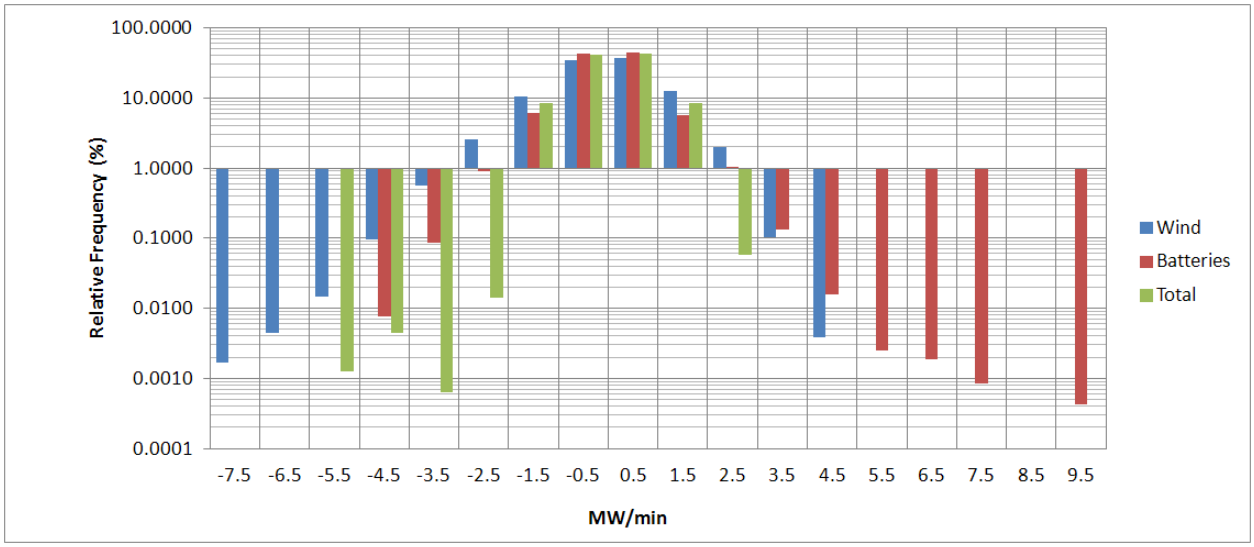

	Relative Frequency of 1-min Ramp Rate Occurrences (%)			Ramp Rate Reduction
Bin (MW/min)	Wind Power[1]	Batteries	Total[3]	Ratio Between Columns 1 and 3
-7 — -8	0.002	0.000	0.000	-
-6 — -7	0.004	0.000	0.000	-
-5 — -6	0.015	0.000	0.001	11.50
-4 — -5	0.096	0.008	0.004	21.67
-3 — -4	0.558	0.086	0.001	884.33
-2 — -3	2.574	0.907	0.014	182.54
-1 — -2	10.343	6.040	8.308	1.24
0 — -1	34.393	42.088	40.581	0.85
0 — 1	37.571	43.961	42.728	0.88
1 — 2	12.372	5.745	8.306	1.49
2 — 3	1.967	1.010	0.057	34.23
3 — 4	0.102	0.135	0.000	-
4 — 5	0.004	0.016	0.000	-
5 — 6	0.000	0.003	0.000	-
6 — 7	0.000	0.002	0.000	-
7 — 8	0.000	0.001	0.000	-
8 — 9	0.000	0.000	0.000	-
9 — 10	0.000	0.000	0.000	-

15 References

[1] HECO. *Draft Request for Proposals for Renewable Energy and Undersea Cable System Projects Delivered to the Isalnd of Oahu.* Draft document. Docket No. 2011-0225. September 28, 2012. www.heco.com.

[2] HECO. *HECO Model Power Purchase Agreement for Renewable Energy Projects.* June 2008. www.heco.com.

[3] HECO. *Kahuku Wind Power Power Purchase Agreement—Interconnection Requirements Study.* Docket No. 2009-0176. February 2010. www.heco.com.

[4] C. Kamath. "Understanding Wind Ramp Events Through Analysis of Histoprical Data." *IEEE Power and Energy Society Tranmsission and Distribution Conference and Exposition Proceedings*; 2010, New Orleands, Louisiana.

[5] H. Zheng and A. Kusiak. "Prediction of Wind Farm Power Ramp Rates: A Data-Mining Approach." *Journal of Solar Energy Engineering* (131), 2009.

[6] A . Florita, B.-M. Hodge, and K Orwig. "Identifying Wind and Solar Ramping Events." Prepared for the IEEE Green Technologies Conference, April 4–5, 2013, Denver, Colorado.

[7] Power Generation University. *An Analysis of Ramping Rates and Dispatch Timing: Matching Renewable Energy and Traditional Energy Generation With Loads.* www.powergenu.com/courses/24/PDF/PGU_AnalysisOfRampingRates.pdf.

[8] K. Coughlin and J. Eto. *Analysis of Wind Power and Load Data at Multiple Time Scales.* Berkeley, CA: Lawrence Berkeley National Laboratory, December 2010.

[9] H. Louie. "Evaluation of Probabilistic Models of Wind Plant Power Output Characteristics." Prepared for the 11th International Probabilitic Methods Applied to Power Systems Conference, June 2010.

[10] D. Lee and R. Baldick. "Limiting Ramp Rate of Wind Power Output Using a Battery Based on the Variance Gamma Process." Prepared for the International Conference on Renewable Energies and Power Quality, March 2012.

[11] A. Esmaili and A. Nasiti. "Power Smoothing and Power Ramp Control for Wind Energy Using Energy Storage." Prepared for the IEEE Energy Conversion Congress and Exposition, September 2011.

[12] D. Lee, J. Kim, and R. Baldick. "Ramp Rates Control of Wind Power Output Using a Storage System and Gaussian Processes," September 2012. www.ourenergypolicy.org/wp-content/uploads/2012/10/1610-Duehee-Lee.pdf.

[13] D.W. Scott. "On Optimal and Data-Based Histograms." *Biometrika* (66:3), 1979; pp. 605–610.

[14] G. Box, G. Jenkins, and G. Reinsel. *Time Series Analysis.* Upper Saddle River, NJ: Prentice-Hall, 1994. ISBN 0-13-060774-6.

[15] E. J. Gumbel. *Statistics of Extremes.* New York: Columbia University Press, 1998. ISBN 0-486-43604-7.

[16] "The R Project for Statistical Computing: The R Manuals." Online resource. www.r-project.org.